# DEVELOPMENT OF AN OPTICAL DISC RECORDER

## QUARTERLY TECHNICAL REPORT

1 October 1976 to 31 December 1976

Sponsored by

DEFENSE ADVANCED RESEARCH PROJECTS AGENCY

ARPA Order No. 3080
Program Code No. 6D30

Contract No. N00014-76-C-0441

Principal Investigator: George Kenney (914) 762-0300
Scientific Officer: Marvin Denicoff

Amount of Contract: $774,900
Contract Period: 1 Oct. 1975 - 31 May 1977









Prepared by

PHILIPS LABORATORIES
A Division of North American Philips Corporation
Briarcliff Manor, New York 10510

February 1977

UNCLASSIFIED

SECURITY CLASSIFICATION OF THIS PAGE (When Data Entered)

## REPORT DOCUMENTATION PAGE

READ INSTRUCTIONS BEFORE COMPLETING FORM

1. REPORT NUMBER

2. GOVT ACCESSION NO.

3. RECIPIENT'S CATALOG NUMBER

4. TITLE (and Subtitle)

DEVELOPMENT OF AN OPTICAL DISC RECORDER

5. TYPE OF REPORT & PERIOD COVERED

Quarterly Technical Report.
1 Oct. 1976 - 31 Dec. 1976

6. PERFORMING ORG. REPORT NUMBER

7. AUTHOR(s)

G. Kenney, F. Zernike, D. Lou, R. Harper, M. Giebler, A. Milch, J. Wagner, A. Chan, R. McFarlane

8. CONTRACT OR GRANT NUMBER(s)

N00014-76-C-0441

9. PERFORMING ORGANIZATION NAME AND ADDRESS

PHILIPS LABORATORIES
A Division of North American Philips Corp.
Briarcliff Manor, New York 10510

10. PROGRAM ELEMENT, PROJECT, TASK AREA & WORK UNIT NUMBERS

ARPA Order No. 3080
Program Code No. 6D30

11. CONTROLLING OFFICE NAME AND ADDRESS

Defense Advanced Research Projects Agency
1400 Wilson Boulevard
Arlington, Virginia 22209

12. REPORT DATE

February 1977

13. NUMBER OF PAGES

72

14. MONITORING AGENCY NAME & ADDRESS (if different from Controlling Office)

Office of Naval Research
800 North Quincy Street
Arlington, Virginia 22217
Code: 437

15. SECURITY CLASS. (of this report)

UNCLASSIFIED

15a. DECLASSIFICATION/DOWNGRADING SCHEDULE

16. DISTRIBUTION STATEMENT (of this Report)

Approved for public release. Distribution unlimited.



17. DISTRIBUTION STATEMENT (of the abstract entered in Block 20, if different from Report)

18. SUPPLEMENTARY NOTES

19. KEY WORDS (Continue on reverse side if necessary and identify by block number)

optical disc recorder
direct read after write (DRAW)
lasers
substrate materials
recording materials
disc protective mechanism
disc

20. ABSTRACT (Continue on reverse side if necessary and identify by block number)

Several air sandwich discs were fabricated and recordings made with them. Tellurium was chosen as the best material of those considered. Studies show that tellurium films are twice as sensitive as bismuth films and are quite resistant to high-temperature degradations. Micron-size pits were recorded in a tellurium film at 2 Mbits/sec with a 25mW He-Ne laser. Extensive tests and evaluations of focus motors and the air bearing sled indicate that an acceptable focus motor and sled can now be integrated into the recorder. Two types of air bearing turntables are now available, including one assembled from standard U.S. manufactured parts. (Cont.)

DD FORM 1 JAN 73 1473 EDITION OF 1 NOV 65 IS OBSOLETE

387 334

UNCLASSIFIED

SECURITY CLASSIFICATION OF THIS PAGE (When Data Entered)

20. ABSTRACT (Cont.)

A Miller modulator/demodulator of digital information was designed, built and successfully tested. A study and computer simulation of the modulator/demodulator is presented.

TABLE OF CONTENTS



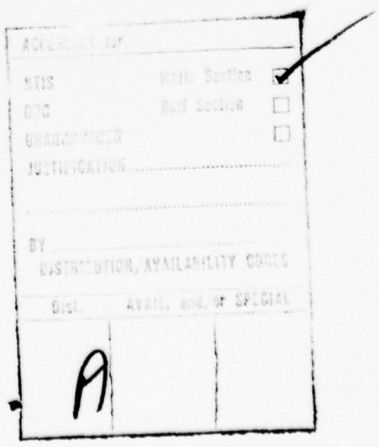

PHILIPS LABORATORIES

QUARTERLY TECHNICAL REPORT
1 October 1976 to 31 December 1976

## 1. SUMMARY

Several air sandwich discs were fabricated and recordings made with them. The air sandwich configuration continues to appear as a practical mechanism for protecting the recording. Tellurium was chosen as the best material of those considered. Studies show that tellurium films are twice as sensitive as bismuth films and are quite resistant to high-temperature degradations. Bismuth remains as an acceptable alternate material. Micron-size pits were recorded in a tellurium film at 2 Mbits/sec with a 25mW He-Ne laser. Extensive tests and evaluations of focus motors and the air bearing sled were completed with the result that an acceptable focus motor and sled can now be integrated into the recorder. Two types of air bearing turntables are now available. The most recent turntable was assembled from standard U.S. manufactured parts. A Miller modulator/demodulator of digital information was designed, built and successfully tested. A study and computer simulation of the modulator/demodulator is presented in Appendix C.

## 2. RESEARCH PROGRAM OBJECTIVES

The objective of this program is to develop an optical disc recorder of digital information, with a direct-read-after-write (DRAW) capability. A storage capacity of $>10^{10}$ bits is desired, with $4.4 \times 10^5$ bits on each of the 40,000 tracks of the disc. The desired error rate is $10^{-9}$ at a data rate greater than 1.33 Mbit/sec. The key element in the proposed system is a recording material that can be exposed with a low-power laser (e.g., HeNe), leading to a recorder that could be manufactured for <$10,000 and discs that would cost <$10 in quantity.

## 3. SCHEDULE

The program schedule and milestones given in Figure 1 are for both materials development and recorder construction. Milestones 3 and 4 were completed by the selection of tellurium as the best material of those considered (Bi, $AsSe_3$, Sb, Cd, Te and Se). The clean room at PL will be operational by mid-February. We expect to produce at least 25 clean air-sandwich discs of tellurium for testing and characterization next quarter. Task 1.3, the evaluation of defects of the clean air sandwich discs, will begin at the end of February with results expected by mid-April. The characterization will be done in cooperation with the Philips Research Laboratories in the Netherlands.

Several experimental air sandwich discs have been fabricated and written in, and refinements of the air sandwich have continued in the areas of fabrication and testing. We are now beginning Task 1.5, the finalization of a working disc design.

Task 1.6 is proceeding well, with the first comparative results of tellurium and bismuth completed (Milestone 14). The program has shown tellurium films to be twice as sensitive as bismuth films and to be quite resistant to high-temperature degradation. The testing program will continue with the additional parameter of humidity stress.

Tasks 2.3 and 2.5 have been somewhat delayed due to the extensive testing and evaluation of the focus motors (Par. 4.0) and the air bearing sled (Par. 4.2). These tests are now complete and assembly of the recorder will proceed with the back-up sled. The optical system should be assembled (Milestone 8) by February 28, 1977, leading to the final system assembly by March 15, 1977 (Milestone 10a). The system checkout is now planned to be completed by the end of April (Milestone 10b). As stated in the last report, these delays are due to re-fitting the recorder around the back-up sled.

Development of the digital electronics subsystem (Task 2.2) is proceeding based on the characterization of bismuth films. The

error encoding, detection and correction systems are conservatively designed to accommodate possible large differences (if any) between tellurium and bismuth films. Two error detection and correction systems should be operational next quarter (Milestone 7b).

Some parametric studies are planned next quarter on the PRL and PL recorders (Task 2.6).

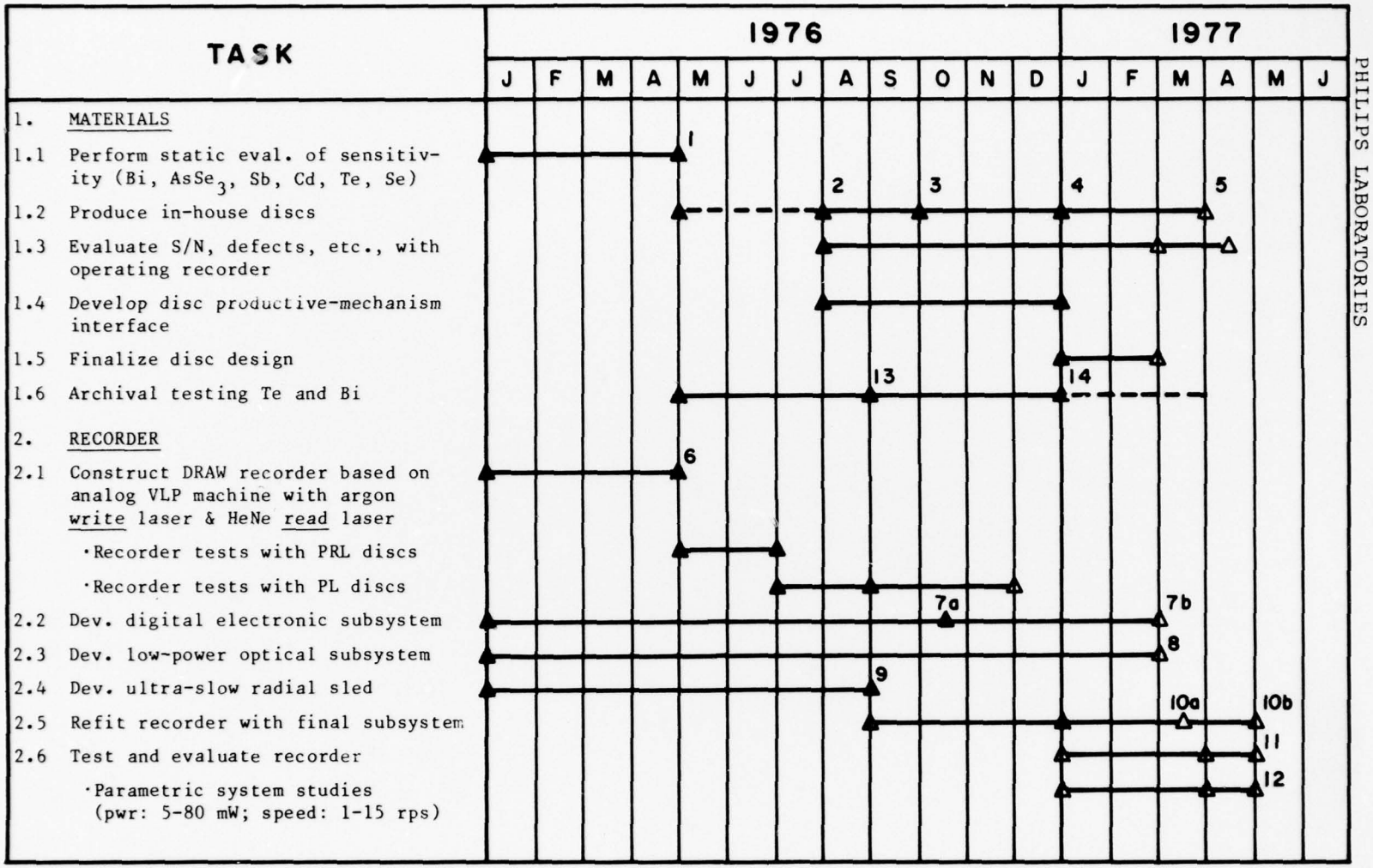


▲ *Completed tasks.*

Figure 1: Program Schedule for Development of Optical Disc Recorder

(Sht. 1 of 2)

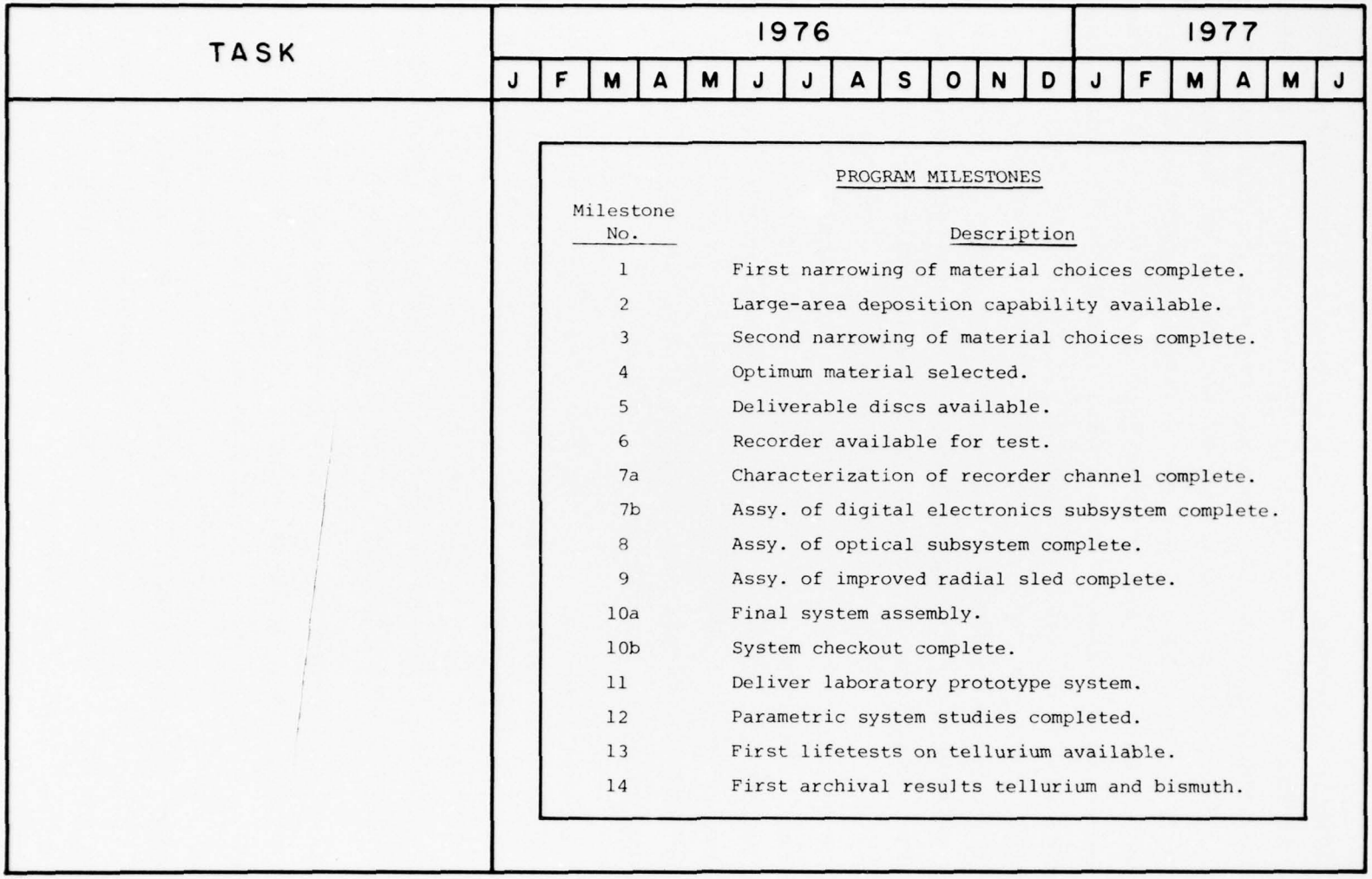


PROGRAM MILESTONES

| Milestone No. | Description |
|---|---|
| 1 | First narrowing of material choices complete. |
| 2 | Large-area deposition capability available. |
| 3 | Second narrowing of material choices complete. |
| 4 | Optimum material selected. |
| 5 | Deliverable discs available. |
| 6 | Recorder available for test. |
| 7a | Characterization of recorder channel complete. |
| 7b | Assy. of digital electronics subsystem complete. |
| 8 | Assy. of optical subsystem complete. |
| 9 | Assy. of improved radial sled complete. |
| 10a | Final system assembly. |
| 10b | System checkout complete. |
| 11 | Deliver laboratory prototype system. |
| 12 | Parametric system studies completed. |
| 13 | First lifetests on tellurium available. |
| 14 | First archival results tellurium and bismuth. |

Figure 1: Program Schedule for Development of Optical Disc Recorder (Sht. 2 of 2)

## 4. SYSTEM CONSIDERATIONS

Discussions with Lawrence Livermore Laboratories personnel and other potential users of an optical disc recorder have uncovered various system requirements which are relevant to the present project. The archival properties of the record are of great importance to some users. These users have even concluded that any erasable materials may be undesirable for their applications. Furthermore, it was stated that a disc recorder with a dual function record/playback sled is undesirable due to the danger of accidental overwriting of information during a read operation. Separate record and playback sleds and playback-only units are considered necessary to insure the record being preserved. Additionally, a single sled recorder is not attractive to the users who wish to access information on a previously recorded track. Of course it is possible for the user to wait until recording is completed. However, in view of the $10^{10}$ bit capacity, the delays may be intolerable. Therefore, from a user's convenience viewpoint, it can be argued that a system consisting of a recorder with separate record and playback sleds, and separate playback-only units, is desirable.

There are other technical reasons for a two-sled system. Primarily, sled specialization will allow each function to be better optimized. For example, the requirements of rapid access may compromise the design of a sled with uniform ultra-slow motion. In another example, discussed in Par. 4.9, a separate recording sled may allow a very simple optical system to be used.

The available recording laser power limits the maximum disc speed and data rate. A 25 mW laser will allow disc speeds of 3 rps and 1.33 Mbit/sec. It would be unfortunate to have the recording laser power limit the performance of the playback mode. For example, a playback-only sled with its own turntable could be made to operate at a higher disc rotation speed. This would increase the data rate (e.g., 10 Mbits/sec) and reduce the disc latency time (17 ms vs. 166 ms).

For these reasons, further consideration will be given to the design of separate sleds for record and playback.

## 4.1 Sleds

The vibration previously encountered in the linear velocity sensor of the sled was traced to crosstalk between the linear motor and velocity sensor, and was reduced by mounting the winding section of the velocity sensor on the moving collar, while holding the magnet in a fixed position. As the location of the winding is shifted along the sled axis, a position for minimum crosstalk between motor and velocity sensor is achieved.

The frequency response of the motor and motor-velocity sensor combination was measured. As expected, the motor behaved as a double integrator and, since the velocity sensor response is proportional to velocity, the combination behaved as a single integrator.

The response at frequencies above 100 Hz showed resonances in the mechanical structure up to 1 kHz and an electrical resonance of the sensor at 20 kHz. The servo response was rolled off at 110 Hz and 400 Hz to control these resonances. Closed loop behavior with this compensation was stable but the system was not particularly effective in correcting low-frequency velocity errors due to friction and cable drag.

To improve the low-frequency response, a lag (integrator) at zero frequency was added to provide essentially infinite dc gain (see Fig. 2). The large low-frequency gain is needed because of the low sensitivity of the motor and tachometer. The tachometer delivers 10 μV per μm/sec. At a nominal sled velocity of 6 μm/sec, a 10% variation in speed results in a 6 μV tachometer error signal. Experimentally, the drag produced by the flexible air hose of the bearing was found to be 0.14 N. Since the linear motor sensitivity is approximately 0.33 N/V (see Fig. 3), a 0.41 V correction signal is required for this error. Therefore, the loop gain must be of the order of 100 dB.

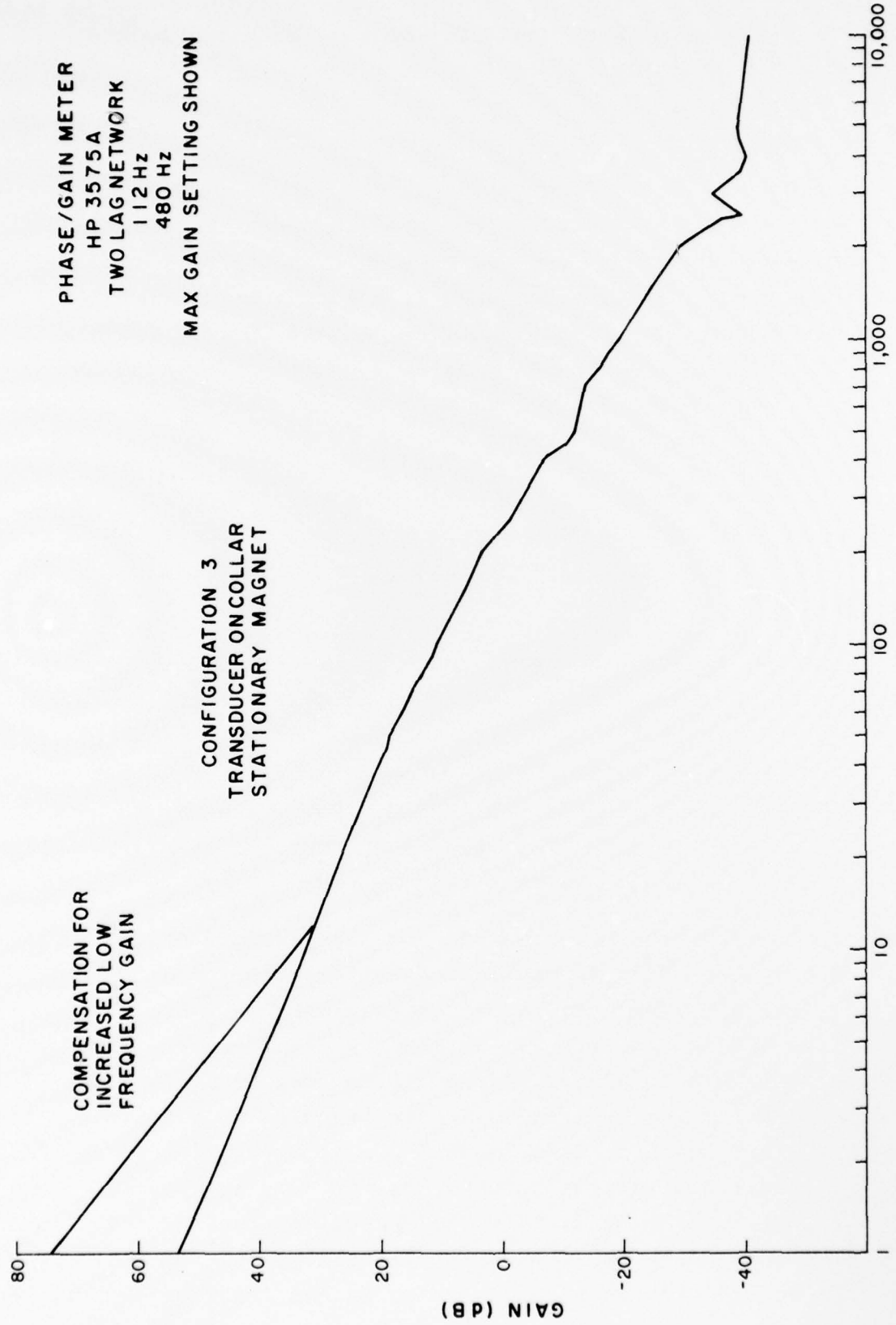


Figure 2: Open Loop Gain of Sled Servo

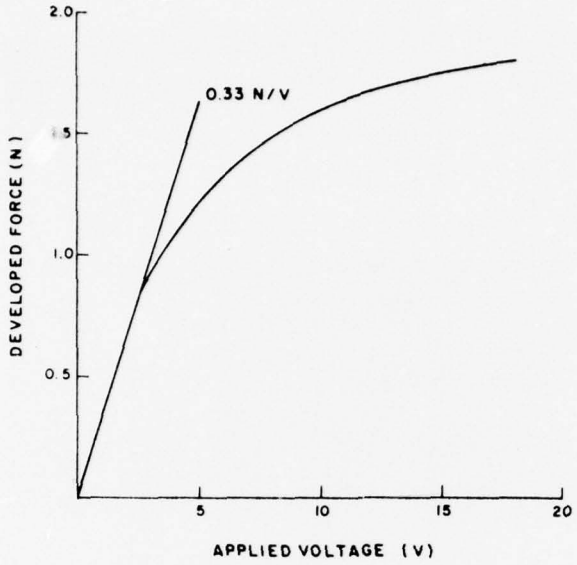


Figure 3: Sled Linear Motor

The closed loop step response of the sled servo is shown in Figure 4. The step was electrically induced and is equivalent to a velocity step of 30 μm/sec at the sled. The rise time of 2 ms corresponds to a 3 dB bandwidth of 170 Hz. This bandwidth appears to approach the maximum realizable from the present mechanical structure since the first significant resonance occurs at 200 Hz. This bandwidth is adequate for the system in the present laboratory environment because the table provides vibrational isolation for frequencies above 1 Hz, and internally the system experiences fundamental vibrations of 3 Hz. The bandwidth requirements of the final unit are not known at this time. A study is planned to determine the full bandwidth requirements of a practical recorder. As the opto-mechanical assembly on the sled progresses, measurements will be made to more accurately define the spectrum of the induced velocity errors.

The sled operates at constant velocities as low as 1 μm/sec. Figure 5 shows the linearity of the velocity at approximately 2.9 μm/sec on a storage oscilloscope. Each trace corresponds to 2.9 μm of travel.

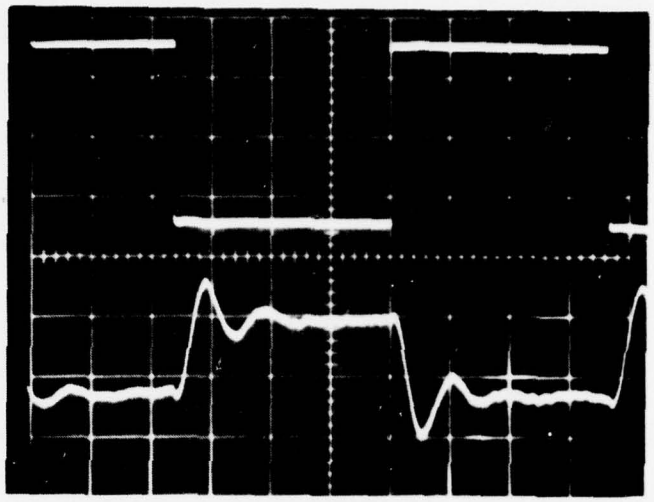


Figure 4: Velocity step response of sled servo.

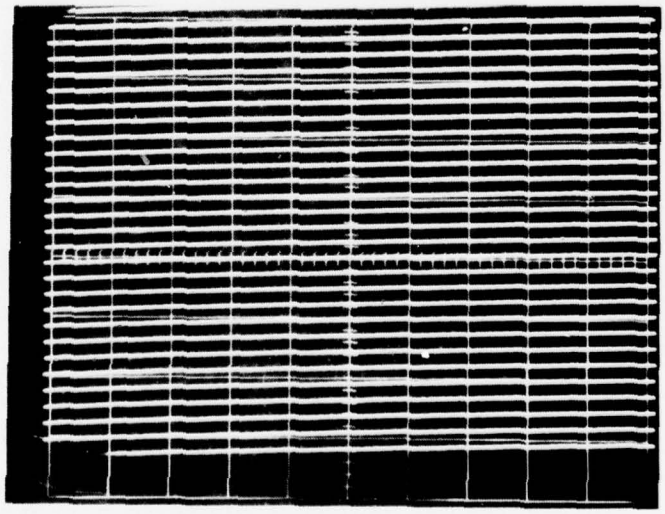


Figure 5: Oscilloscope trace of sled velocity over a limited range.

Conventional "wisdom" has until now taught us that sleds employing air bearings driven by induction motors are the best and possibly unique solution for uniform ultra-slow motion. Additionally, the philosophy at the onset of the project was to require the sled to be capable of rapid access. If both conditions are required, then it appears that there are no alternatives to air bearing sleds. However, in view of the shifted approach to employ two sleds, each optimized for a particular function, it seems prudent to examine alternate approaches to ultra-slow motion sleds.

One alternate approach to a slow speed sled is based on a lead screw drive; therefore, construction of a lead screw sled was begun. The sled itself is an aluminum carriage that slides on teflon buttons in a V-groove ground in steel. It is driven by a precision lead screw with a pitch of 2.54 mm, made by Universal Grinding Corporation of Fairfield, Connecticut. The screw is driven with a 360:1 gear rate by an adjustable-speed dc motor-generator. The performance of the lead screw sled will be compared to the air-bearing sled and reported next quarter.

## 4.2 Focus Motor

Three focus motors were evaluated as planned. The response of the PL, PRL and integrator player focus motors is shown in Figure 6. Resonances and limited range eliminated the PL and integrator player motors from consideration. The PRL motor was chosen because it has a working range of $\pm$ 1.0 mm, a smooth frequency response, and an acceptable sensitivity. The required working range is $\pm$ 1.0 mm; the required frequency response is 2 kHz. A more complete description of the focus motors' behavior is given in Appendix A.

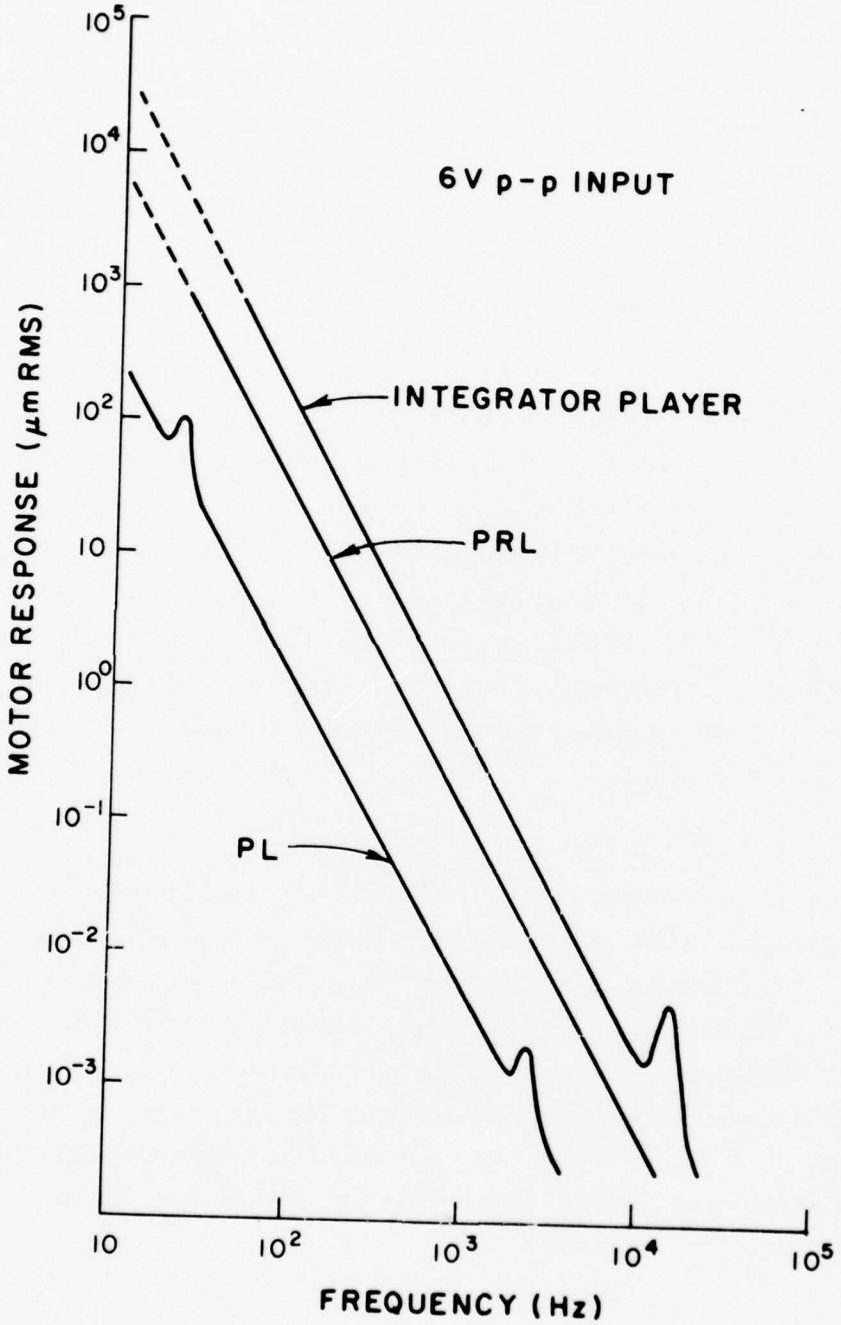


Figure 6: Frequency response of focus motors of three systems: the integrator player, PRL writer, and PL writer.

## 4.3 Air Bearing Turntables

Testing of the ac-drive turntable revealed that the air bearing was subject to galling at 30 Hz under low or no-load conditions. Modifications were made to the spindle and sleeve. The indication thus far is that the problem has been corrected without measurably affecting the air consumption, stiffness or wobble. The radial wobble of the spindle is less than the required 0.1 μm at 30 Hz. Wobble measurements have yet to be made at 3 Hz.

The dc-drive turntable components were built, and the turntable was assembled (see Fig. 7). It consists of a Kollmorgen Corporation pancake armature motor (Type U9M4) with the ball bearings removed and replaced by a Professional Instruments'

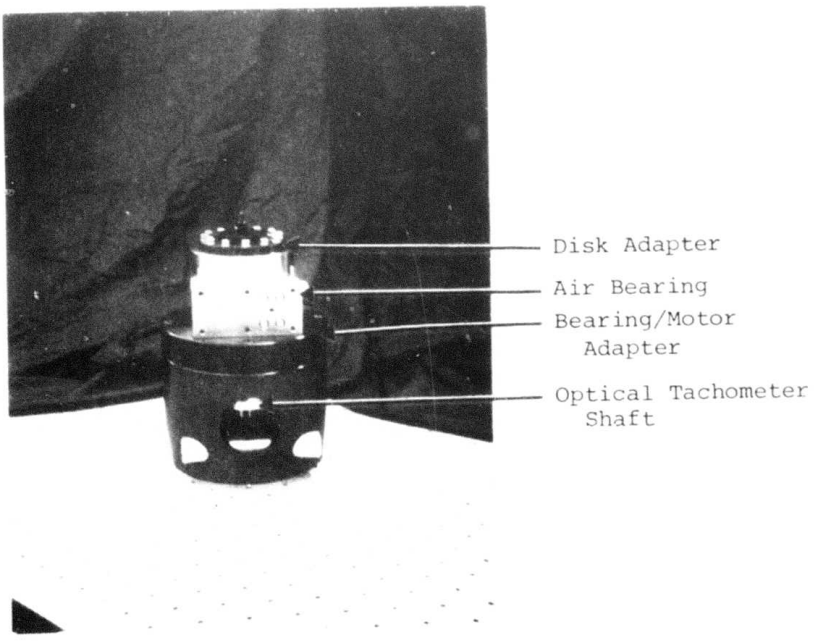


Figure 7: dc-drive turntable

rotary air bearing (Model 4B). The air bearing has been directly coupled to one end of the motor shaft. A 2000-line optical encoder dial and single pick-off were mounted on the other end of the motor. Evaluation of the electro-mechanical characteristics of the turntable has begun. At 3 rps, the radial wobble of the spindle at the disc adaptor is less than the resolution of our equipment (<.05 μm). Results are not yet available for 30 rps operation.

## 4.4 Materials Evaluation

A Model 907 He-Ne laser was received from Spectra Physics. Output was found to be 25 mW in the $TEM_{\infty}$ mode. Micron-size pits were machined on 300-Å thick Te films deposited on PIBMA (polyisobutyl methacrylate) coated glass masters. Modulation was provided by a Harris Model 180 acoustoptic modulator. Pulse duration was approximately 500 nsec; disc rotation speed was 6 rps. Figure 8 shows a picture of the pits taken through an optical microscope.

Test recordings have also been made on a PMMA air sandwich coated with Te films (on one side). Figure 9 shows optical microscope pictures of recorded pits. Although no direct reading after writing was attempted in this experiment, it is believed that the pit profiles shown here would be more than adequate for playback in the digital format. No significant deposit of tellurium was observed on the opposite side of the air sandwich, except when recording was done at extremely high power with a duty cycle of 100%. We therefore conclude that interference between the two faces of an air sandwich would not be likely.

To summarize our results to date, static measurements have shown that Te films are a factor-of-two more sensitive than bismuth. Theoretical calculations show that under optimum conditions (Ref. 1), these films should have adequate dynamic sensitivity for recording at 2-5 Mbits/sec with a 25 mW He-Ne

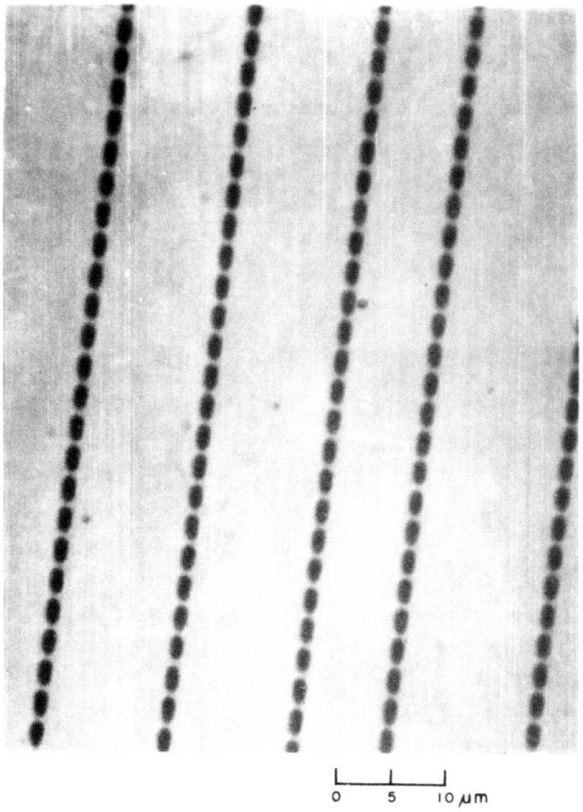


Figure 8: 25 mW HeNe laser on 300 A Te on PMMA-coated glass master. Disc rotation speed approximately 400 rpm.

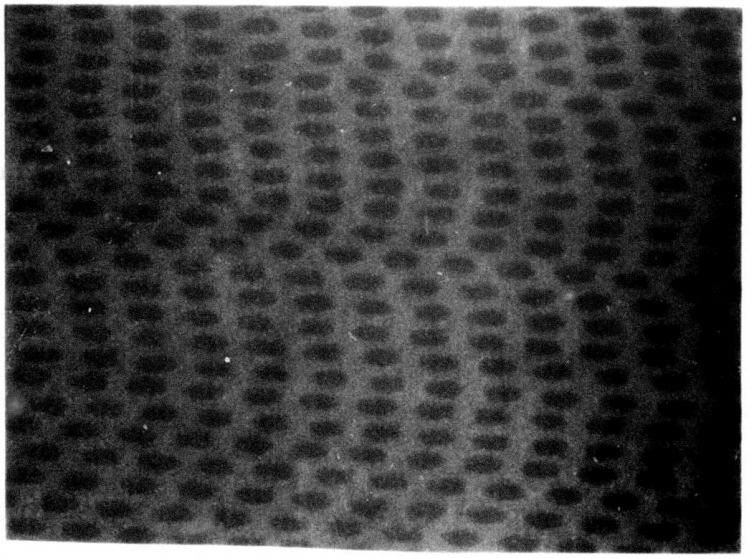

Figure 9: Pits recorded in a tellurium-coated air sandwich (magnification 2000X).

laser. Micron-size pits have been recorded at 2 Mbits/sec with a 25 mW He-Ne laser. An archival testing program has shown these films to be quite resistant to degradation. The feasibility of methods to protect and contain the recording appears to have been demonstrated with the air sandwich disc structure. It seems highly likely that tellurium would be an acceptable recording material for use with a 25 mW He-Ne laser at 2 Mbits. Further materials effort will concentrate on the continued development and improvement of tellurium. These efforts should result in optimization of the writing properties of the tellurium films, such as repeatability of hole shape and defect densities.

### 4.5 Air Sandwich Disc

Activities on the air sandwich disc have continued. The principal efforts have been refinement of the assembly technique, measurement of the static and dynamic profiles of the disc film plane, optimization of the disc dimensions, and investigation of alternative substrate and disc fabrication methods. Several discs were fabricated for evaluation and one was written in (see Par. 4.4).

The problem of non-uniform spreading (Ref. 2) of the adhesive during lamination was solved by making three modifications to the assembly technique. First, the surfaces of the base and vacuum hold-down plates in the assembly fixture were made more compliant (softer). As a result, we feel the contact pressure--applied to the adhesive during the curing cycle--was made more uniform. Second, the ratio of the volume of adhesive dispensed in the two standoff zones was changed. This modification, which resulted in a more nearly equal adhesive thickness in the inner and outer standoff zones, also tended to make the contact pressure more uniform throughout the adhesive. Finally, the contact pressure applied during the curing stage was increased from about 1 psi to about 5 psi. Several additional modifications to

our technique and to the assembly fixture are currently being incorporated in order to further improve the bond quality and disc flatness.

Measurements on many more discs are required before we can fully characterize the average static and dynamic film plane profiles. In particular it is important to measure the axial deflection of the disc due to gravity, called droop, where the disc is resting on the turntable spindle. The droop of the outer edge of the disc establishes the necessary travel of the focus motor. Measurements currently show a droop of about 0.75 mm. It is also essential to have statistically meaningful measurements of the axial deflection of the film plane of the disc while it is spinning at the operating speed of 3-4 rps. This information establishes the bandwidth required of the focusing motor and its control loop. Although the existing measurements are insufficient to establish a bandwidth specification, at 3-4 rps the focusing servo of the machine should have no difficulty in following the film plane. In addition to accruing short-term data, detailed measurements of the creep behavior* of the air sandwich discs has now begun.

Optimization of the disc dimensions is well underway. There are four specific areas of consideration: cavity thickness, spindle hole diameter, turntable support surface, and static balancing. In view of the fact that the disc may also be spun at 30 rps, it is worthwhile to consider a disc design capable of both 3 rps and 30 rps operation. At the present time it does not appear that the dimensions and fabrication of a dual speed disc would be significantly different from a disc intended strictly for 3 rps operation. The primary differences are in the cavity thickness and balance requirements. The cavity thickness, required to prevent the film planes from touching while spinning, depends on such things as the inside diameter of the cavity,

---

* *The axial and radial deformation of the disc when it rests on a turntable, or spins at high speed, for periods of time equivalent to many record and playback sessions.*

and the turntable support dimensions as well as the speed of operation. The inside diameter of the cavity and the turntable support dimensions are in turn set by other subsystem considerations such as the dimensions of the sled and focus motor. Current estimates are that the inner cavity diameter and the outer diameter of the disc adapter on the turntable can be set as large as 6.5 cm and 3.8 cm, respectively. Under these conditions the disc is so stiff that the theoretical cavity thickness required even for 30 rps operation is less than the typical unflatness (0.1 - 0.2 mm) of the film plane. The net result is that the cavity thickness can be selected by the practical desire to prevent contact of the films during "normal" handling of the disc. At present, the cavity thickness required for such a purpose is 0.25 - 0.5 mm. The static balance requirement is much more severe for high-speed operation than for low-speed. However, we have discovered that by locating the center of gravity after the disc is fabricated, then finally drilling the spindle hole, the disc is balanced to within 2-5 gm-cm. This amount of imbalance is not expected to be of any consequence at 30 rps.

Excessive variations in substrate thickness have been of some concern (Ref. 3). Such irregularities make it difficult to compensate the light path. In addition, they cause variations in local stiffness, giving rise to irregularities in the axial deflection of the film plane around the circumference. The problem of thickness variations, in excess of the normal manufacturer's specification ($\pm$ 12.5%), was discussed with officials of the Glasflex Corporation. An agreement was reached which should result in a considerable improvement in quality control (see Appendix B).

A second source of optical-quality 1 mm thick PMMA was found. Rohm and Haas Corporation casts such sheet but generally only in large volumes. In cooperation with PRL, we have been able to secure a regular allotment of the material. The samples received to date are more uniform in thickness than the Glasflex Electroglas Sheet ($\pm$ 4% as opposed to $\pm$ 13%).

An additional potential source of PMMA sheet has also been identified. Apparently Swedlow Corporation manufactures optical quality sheet for aircraft window applications. We are currently investigating the possibility of procuring material from them.

An investigation of alternate--and more mass-production oriented--ways of fabricating substrates and discs was initiated during the quarter. Four specific inquiries are under way. They are: the feasibility of die cutting the substrate and standoff from sheet stock, the feasibility of ultrasonically joining the air sandwich components, the cost considerations of injection molding the substrates, and the feasibility and cost considerations of joint configurations which would allow periodic disassembly of the air sandwich. Results of these inquiries should be available the next quarter.

### 4.6 Life Testing of Tellurium and Bismuth Films

Testing of the aging characteristics of films, as reported previously, continues. Maximum aging time as of the end of 1976 is in excess of 4,000 hours (Ref. 4). About fifteen new sample sets were created during the current quarter, bringing the total number of sets to over 40 and the total number of samples under life test to approximately 250.

Static hole-burning sensitivities are in substantial agreement with the result reported in the previous quarter. That of tellurium is about 300 $mJ/cm^2$ while Bi requires 600 to 700 $mJ/cm^2$ for 1 μm holes. The exposure times were 500 ns for bismuth and 750 ns for tellurium. The power was 3 mW for tellurium and 10 mW for bismuth. Optical transmission appears to be increasing somewhat, but not as yet enough to influence optical absorption significantly. Temperature-humidity testing of tellurium films is planned for the next quarter.

## 4.7 Characterization of Disc Errors

An interchangeable modular system for the characterization of error mechanisms in optical disc systems is being designed and implemented in both hardware and software. Its minimal configuration will consist of a Linkabit LF1011-256 Convolutional Encoder Feedback Decoder and a Miller modulator-demodulator designed and constructed at Philips Laboratories, suitably interfaced into a large minicomputer (SEL 32/55) that will be used to gather real-time error statistics. The maximal configuration will involve fully interchangeable hardware and software modules capable of simulating recorder-player design configurations in addition to gathering and graphically presenting error statistics.

A block diagram of the modular error characterization system is shown in Figure 10. Each block is implementable either in hardware or software and, when constructed in a modular fashion, allows the designer to change system blocks (and/or parameters) in a simple manner. The coder introduces redundancy in a structured manner so as to facilitate detection and correction of random channel errors. Hardware modules for BCH and convolutional codes will be available in addition to the Linkabit system. Software modules for a wide selection of codes are being written. The interleaver reorganizes the coded data so as to facilitate detection and correction of error bursts. A "column" interleaver is being hardware-implemented by GAC (Ref. 5); more complicated interleavers will be implemented by software. The modulator matches the data spectrum to the spectral requirements of the recording/reading process. Candidate modulations (Ref. 6) to be available in software include NRZ (non-return to zero), Manchester, GCR (group coded recording), Miller, and modified Miller.

The recording/reading process may be either simulated by a measured channel transfer characteristic to which is added a

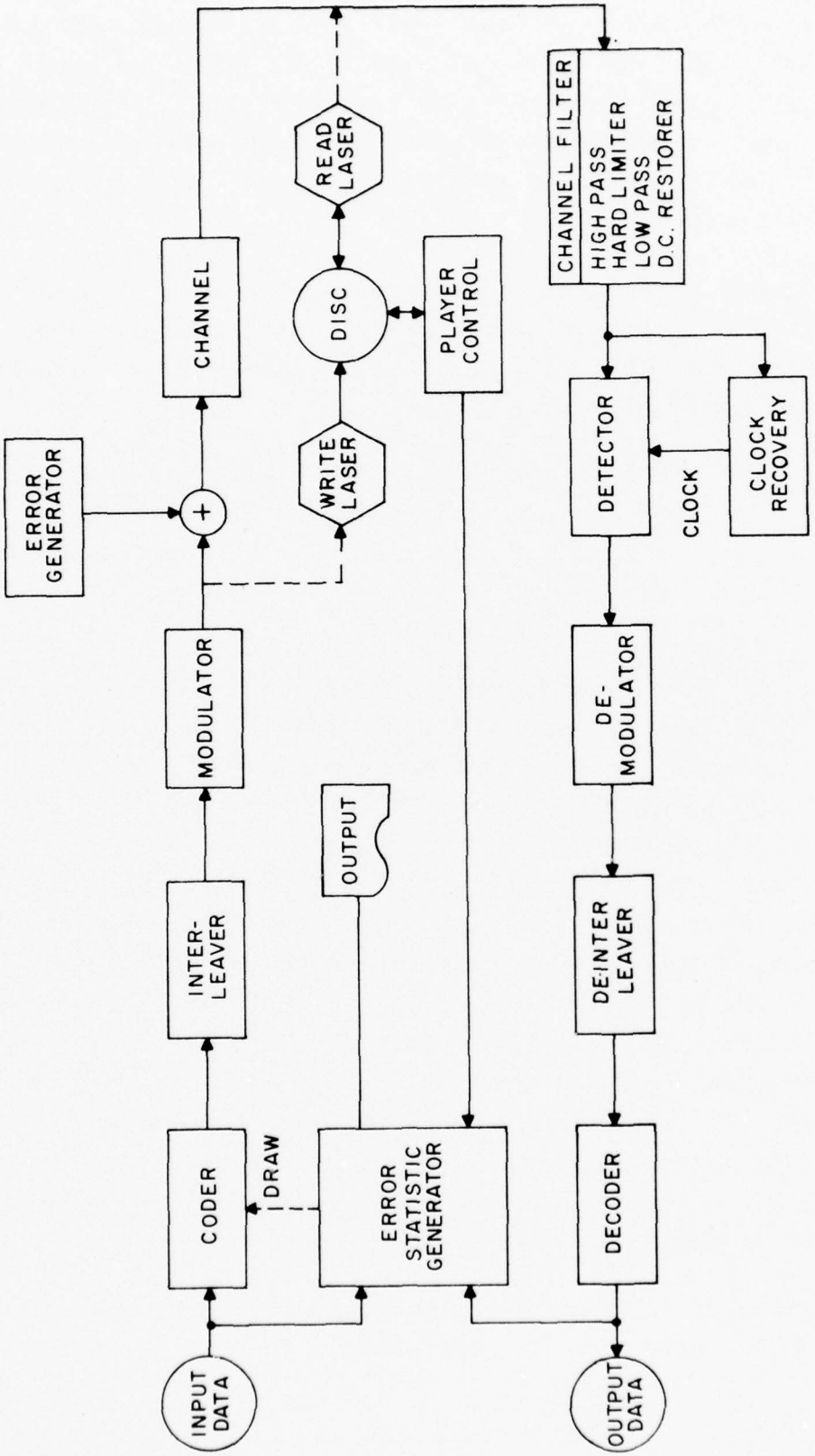


Figure 10: Block diagram of the modular error characterization system.

signal error representing disc eccentricity, rotational speed fluctuations, disc surface and material defects, and laser noise, or directly implemented by the write laser, disc, read laser branch. Increased understanding and identification of error-causing mechanisms will be attained by direct comparison of the alternate approaches.

In a similar manner, channel filters (including high pass, low pass, hard limiters, and dc restorers), detectors, and clock recovery circuits will be modular and implemented in both hardware and software.

The error statistics generator will functionally operate on the decoder output data to determine the error distribution. These may be ascertained from the disc itself or by real-time comparison of the input and output data files.

## 4.8 Digital Channel Modulator/Demodulator and dc Restorer

A Miller modulator and demodulator were designed and debugged with the exception of the PLL (phase locked loop) for which more evaluation and optimization is in progress. The Miller code was chosen to match the user's input data power spectrum to the channel response of the optical disc (Ref. 6). The Miller Modem (modulator and demodulator combination) has been tested working E to E (electronics to electronics) at data rates up to 2.5 Mbps. During read-back a string of 200 synchronizing bits is required for the PLL to lock on. This number of bits is determined by the loop bandwidth (~5kHz). After the synchronizing bits, at least one 101 data sequence should be present to start up the Miller demodulator. A block and timing diagram of the Miller demodulator is shown in Figure 11; the waveform of the Miller Modem is shown in Figure 12.

A dc restoration circuit, using positive feedback, has been designed and tested E to E. The circuit enables playback data

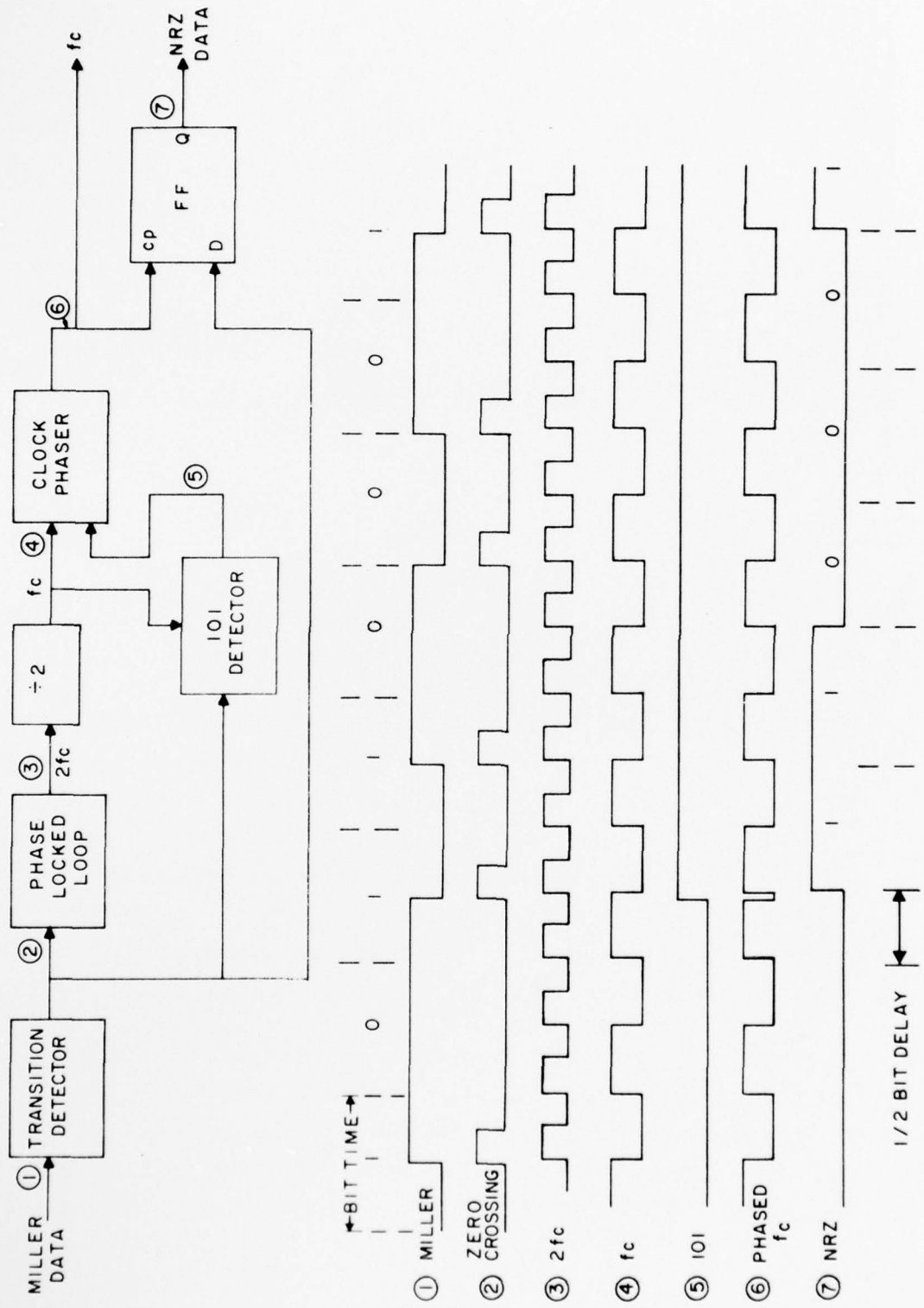


Figure 11: Block and timing diagrams of Miller demodulator

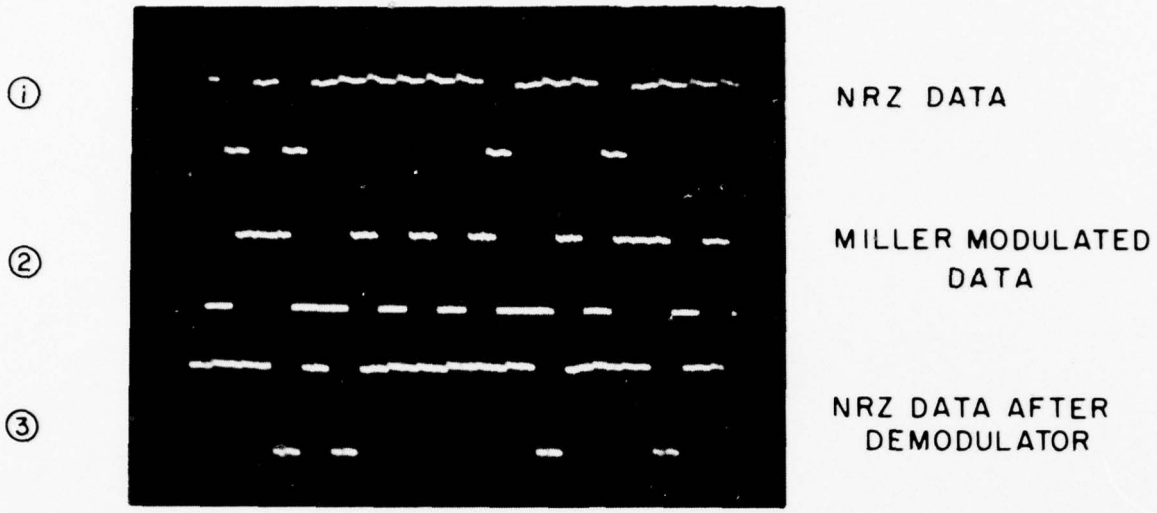


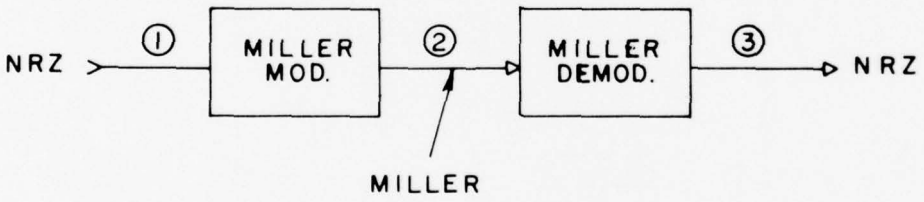


Figure 12: Miller Modem diagram and waveforms.

to be recovered more reliably. A block waveform diagram of this circuit is shown in Figure 13.

Magnavox has done a study with computer simulation on the channel Miller modulator and demodulator and data recovery. The simulation results indicate that the demodulator and PLL considered will provide excellent performance for the distortion conditions simulated (see Appendix C).

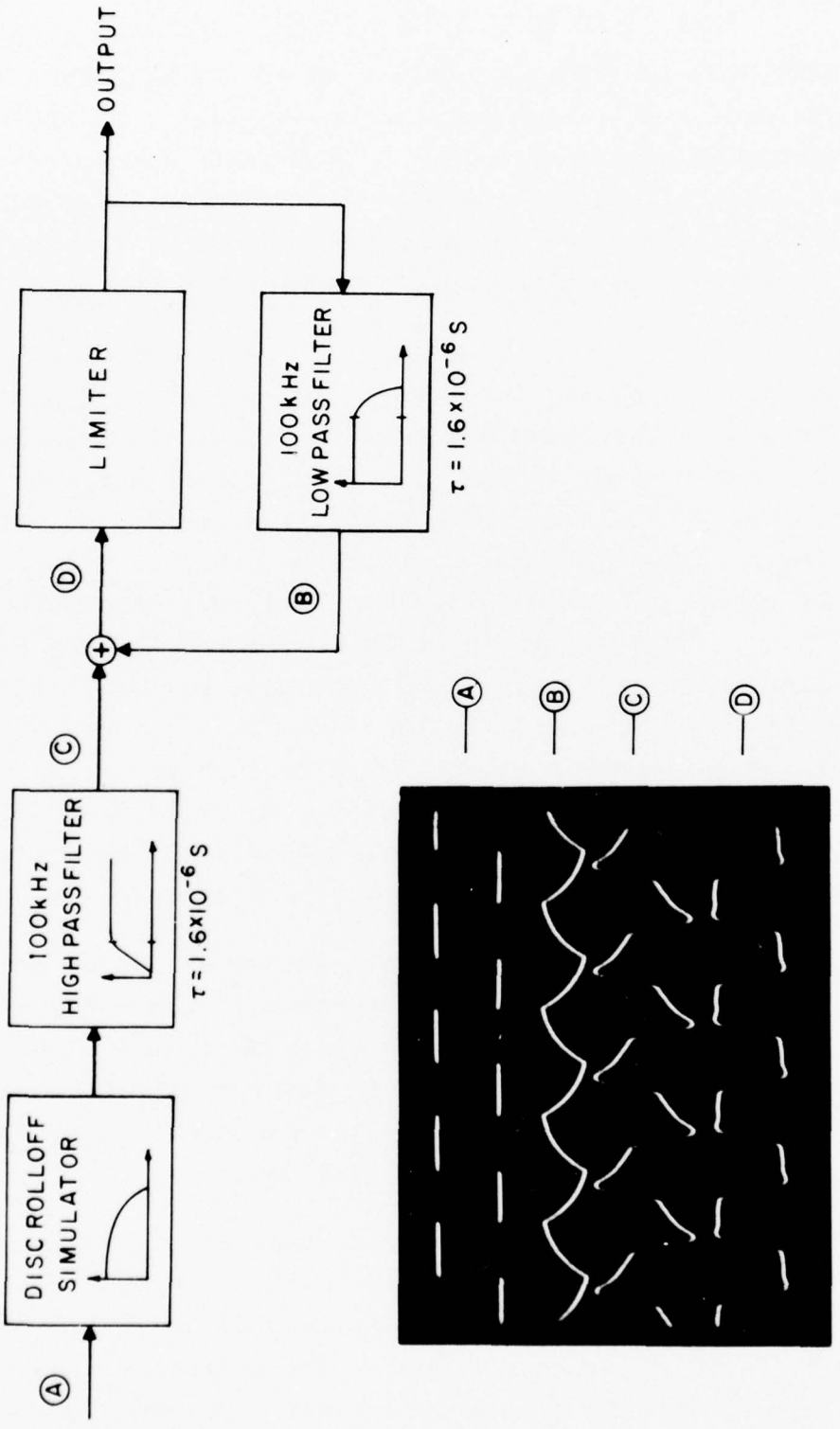


Figure 13: Diagram and waveforms of dc restoration circuit.

## 4.9 A Simplified Recording/Readback Technique

The present DRAW recording technique under investigation requires two lasers and/or a complex optical system to record and playback information simultaneously. An alternate record/readback technique which eliminates the need for a second laser and greatly simplifies the optical system is under study. The new system called "verify during write" monitors the reflected light of the recording laser.

Since some finite amount of exposure time is necessary before a hole is formed by the recording beam, it should be possible to verify the formation of a hole, i.e., the registration of a data bit by monitoring the character of the light reflected from the disc during writing. Assume, for example, that the disc is illuminated by a pulse t seconds long and that it takes T seconds to form the hole. Then, if the hole is indeed formed, the reflected light will have a large value for T seconds, but will fall to a low value (due to the reflectivity of the bare substrate) during the remaining t-T seconds before going back to zero. If a hole is not formed, the amount of reflected light will remain large, whereas if a hole was already there, only a small amount of light will be reflected during the entire t seconds.

An experiment was performed, and this theory was found to be valid. It was found that a small decrease in the reflected light was detected for light levels where only an incomplete hole or "dimple" was formed. Then to discriminate between "dimple" and hole formation, it appears necessary to monitor the level to which the reflected signal decreases.

These preliminary experiments indicate that a verify-during write, rather than a read-after-write mode, is a possibility. However, further experiments are necessary to ascertain the feasibility of the method, including the necessary electronics. In addition, the verify signal is generated by the write beam, i.e., by a beam that is inherently in focus and on track. Thus,

it remains to be proven that a data stream verified as "recorded" by this method can indeed be read back later by a separate reader with equal fidelity.

## 5. PLANS

a. Test lead-screw drive for sled.

b. Assemble optical system.

c. Assemble recorder on back-up sled.

d. Begin humidity testing of tellurium.

e. Fabricate and test first clean air sandwich discs.

f. Finish evaluating Kollmorgen/Professional Instruments turntable.

g. Construct software and hardware modules for characterization and correction of error mechanism.

h. Design separate playback sled/system.

i. Test and verify record/readback scheme.

## 6. REFERENCES

1. See Appendix C, July-Sept. 1976 Quarterly Technical Report.

2. Par. 4.5, July-Sept. 1976 Quarterly Technical Report.

3. Par. 4.6, July-Sept. 1976 Quarterly Technical Report.

4. Par. 4.7 and Appendix D of July-Sept. 1976 Quarterly Technical Report.

5. General Atronics Corp., Subsidiary of Magnavox Government and Industrial Electronics Co.

6. "Optimal Codes for Digital Magnetic Recording," J.C. Mallison and J.W. Miller, IERE Conf. Proc. No. 35, June 1976.

# APPENDIX A

## Evaluation of Three Focusing Motors

## EVALUATION OF THREE FOCUSING MOTORS

The evaluations of the PL and PRL focus motors were completed and compared to the focus motor of the integrated player. The suspected resonance at about 2 kHz for the PL focus motor was confirmed, and it was found to have little response above about 4 kHz. This resonance and low sensitivity may be due to the spring suspension or other mechanical features. A resonance was also found in the PL motor at about 35 Hz.

The PRL motor was found to roll off continuously in amplitude with frequency to at least 12 kHz with no resonances. The PRL bearing and lens assembly is heavier and has a weaker magnet and, therefore, is less sensitive than the integrated player motor. Both dc and ac measurements have shown that the PRL is 3 to 4 times less sensitive.

Mechanically, the PL motor is not satisfactory since its limited travel (about 400 μm) is not sufficient to allow for the droop of a plastic disc, especially at 3 rps. The static droop of a plastic disc is about 0.75 mm. Therefore, a travel range of ± 1.0 mm is required of the focus motor. The air bearing in the integrated player motor was judged to be too loose for recording application. It was therefore decided that the PRL focus motor be used without modification since it exhibited no resonances, has a stiff air bearing, and is acceptably sensitive.

Figure 1 shows a comparison of the response of the three focus motors. The data has been normalized to a 6 volt peak-to-peak input for each motor, although the tests were not all conducted at this voltage. The amplitude of motion was found to increase proportionately with input voltage. The vertical position of the PL motor plot is based on an estimate obtained from a dc sensitivity measurement that showed the PL motor to be about 100 times less sensitive than the integrated player motor. All tests were performed with the motors operating vertically, against gravity. Any amplitude above about 1 mm on the graph is not realistic since none of the motors are capable of such

large travels. This data was scaled from results at drive levels less than 6 volts.

The working range of the PRL motor is ± 5 mm, the PL motor, ± 0.2 mm, and the integrator player, ± 0.5 mm.

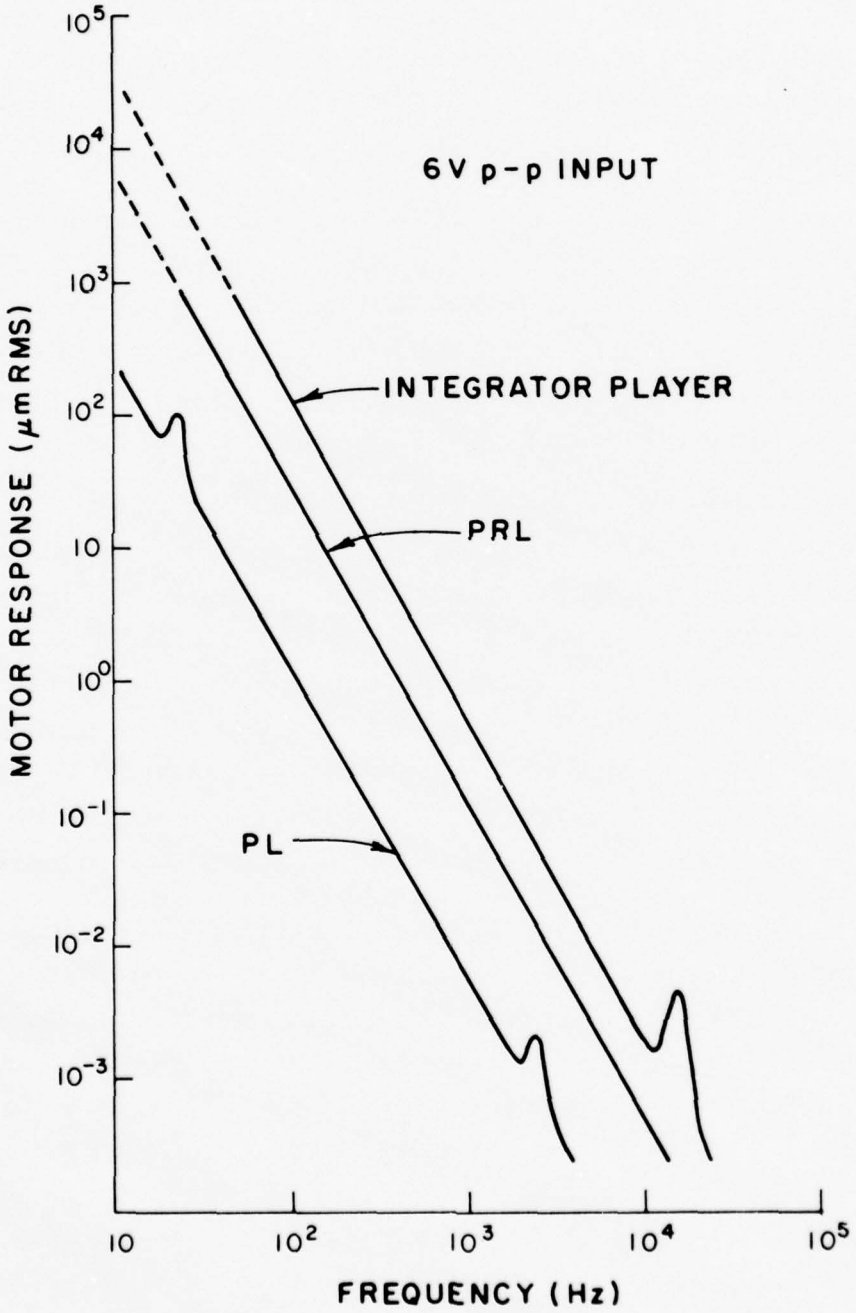


Figure 1: Frequency response of focus motors of three systems: the integrator player, PRL writer, and PL writer.

PHILIPS LABORATORIES

# APPENDIX B

## Trip Report: Glasflex Corporation, Stirling, New Jersey on 15 October 1976

by

A. Milch
J. G. Wagner

PHILIPS LABORATORIES

TRIP REPORT: GLASFLEX CORPORATION,
STIRLING, NEW JERSEY ON 15 OCTOBER 1976

On October 15, 1976 A. Milch and J. G. Wagner visited with the management of Glasflex Corporation in Stirling, N.J. The primary purpose of the trip was to review with Glasflex officials the large thickness variations we have noted in their recent shipments of unmasked Electroglas 500 CT sheet and to agree upon some satisfactory manner of dealing with the problem.

Several samples of 0.040" Electroglas 500 CT sheet were returned to Glasflex for examination. Their inspection indicated that many sheets were within the tolerance band of $\pm$ .005" but the thickness was too large. They felt certain they understood what production parameters needed to be changed in order to insure that the specifications would be met in future production runs. In addition, we agreed that in the future, every fifth sheet would be masked with polyethylene and calibered.

Several other points were discussed in some detail.

- Glasflex Corp. has done some development work for a third party. In particular, they have developed the technology to cast 15" x 15" x .040" acrylic monomer sheets with a tolerance of $\pm$ 0.001" on the thickness. The normal 500 CT tolerance is $\pm$ 0.005". The cost to the third party at the time (approximately 2 years ago) was about $3.00 per sheet.

- In general, Electroglas Sheet does not exhibit a wedge-shaped thickness profile. Sheets that do have a wedge shape are coincidental. It is much more common for a sheet to be thicker in the center than around the edges.

- One of the best ways of bonding Electroglas homopolymer sheet is to use the unstabilized acrylic monomer. We were given a one-quart sample for trial use in the assembly of air sandwiches.

- Rohm and Haas manufactures a two-part adhesive (trade number 96) which works very well with Electroglas sheet.

- Schwartz Chemical Co., Inc., 5001 Second Street, New York also manufactures a good acrylic cement (trade number H-94).

- Glasflex's experience in bonding their copolymer is that the cyano-acrylates are about the only useful adhesives.

- Fusion appears to be an attractive way of joining air sandwich components. However, development of the proper hardware and techniques may require considerably more effort than using adhesives.

- Techniques exist for removing scratches. They are:

  a) Buffing with special compounds (Xpel buffing compound or Dupont #7 Auto Polish).

  b) Flame polishing. This is very much an art, but if we can master it, it sounds ideal for our purpose. Thermoforming temperature range is 210°F ot 230°F.

- Their best cleaning agents are the supermarket type liquid laundry detergents such as All. This is more or less in line with our feelings.

- The homopolymer is a linear molecule; the copolymer is crosslinked with a proprietary copolymerization agent. Both are thermoplastic, but the copolymer does not accept adhesives and they never bond to it. We ought to stay away from it, especially since our original interest in it--its resistance to organic solvents during cleaning--has faded.

# APPENDIX C

## Modulator/Demodulator Design Study for the P.N.A.* Draw Disc

(Report No. 2838-3118-2 Jan. 1977)

by

Robert C. Harper

General Atronics Corporation
*a Subsidiary of*
The Magnavox Government and Industrial Electronics Co.
Philadelphia, PA 19118

*Designation P.N.A. in this report should be read as "optical."

## 1.0 INTRODUCTION

This report describes the analysis carried out to determine the performance of the "Miller" technique for modulating binary information into the P.N.A. Draw Disc. More specifically, the report is concerned with the analysis (via Monte Carlo computer simulation) of a demodulator for extracting the original binary information from the waveform read from the disc.

In case the reader is not familiar with the Miller modulation technique, it is a cute way of remapping a binary (two-level) NRZ data waveform into another binary waveform in which level changes are guaranteed to occur at some minimum rate (regardless of the data). In particular, if the duration of one NRZ data bit is $\tau$ (we refer to the duration, $\tau$, as a "baud"), then in the resulting Miller waveform, we are guaranteed that no two level transitions are separated in time by more than $2\tau$. Furthermore, we note that the Miller waveform requires very little more bandwidth than the original NRZ waveform.

The "rules" for creating a Miller waveform from NRZ are as follows:

a) A logic 1 corresponds to a level transition in the *middle* of a baud.

b) A logic 0 corresponds to a level transition at the *end* of a baud *unless* the logic zero is the *last* of a string of consecutive zeroes. In this case it is simply ignored (i.e., no transition at the end of a final zero). Note that a single isolated zero can be considered as a string of length 1 and is therefore ignored.

One should note from the above set of rules that the Miller waveform contains one bit of information per baud and is, therefore, as "efficient" as the NRZ waveform.

Because the laser used to read the disc has considerable low frequency noise, the resulting waveform must be highpass filtered before being demodulated. The laser proposed for the P.N.A. Draw Disc requires that the corner for this highpass filter be located at 20 kHz. In the analysis to be described, a two-pole Butterworth highpass filter with a 20 kHz cutoff was used for this purpose. Because of this highpass filter, the filtered waveform has no DC component. Consequently, demodulation is very difficult unless one can guarantee some minimum rate

of occurrence of level transition of the unfiltered waveform. We selected the Miller modulation technique for this reason, as well as for the fact that it allows us to maintain an efficiency of one bit per baud. The price paid for these nice features is a small increase in demodulation complexity (resulting from a timing ambiguity inherent in the Miller technique) which will be discussed later.

In addition to the highpass filter just mentioned, we wish to include in our analysis two additional sources of distortion of the waveform read from the disc. These are:

a) The lowpass filtering effect which results from the finite width of the read beam as it passes over the finite length pit.

b) Variation in the data rate read from the disc which results from disc eccentricity.

In Section 2 of this report, we describe the considerations that were made for modelling the effects of (a) and (b) in the Monte Carlo simulation.

Demodulation of the distorted waveform obtained from the disc is accomplished by a circuit which consists of essentially two parts: (1) a detector which reconstructs logic 1's and 0's from the distorted waveform, and (2) a phase locked loop (PLL) circuit which locks to zero crossings of the distorted waveform and provides the necessary timing signals to the detector. Considerations for modelling these two portions of the demodulator are given in Section 3.

The simulation results are presented in Section 4, and, by way of summary, we note that the proposed demodulator has been shown to reconstruct error-free NRZ data from the distorted Miller modulated waveform obtained from the disc. Finally, in Section 5, we describe some special aspects of the modulation/demodulation hardware specifically as it related to the removal of the inherent timing ambiguity associated with a data clock extracted from the Miller waveform.

## 2.0 MODELLING OF WAVEFORM DISTORTION

The first source of distortion indicated in the previous section (i.e., highpass filtering with a two-pole Butterworth filter to eliminate laser noise) needs no further description. Beam convolution and disc eccentricity are discussed below.

### 2.1 CONVOLUTION OF READ BEAM AND PIT

The Miller modulated waveform, when written onto the disc, causes a pit to occur whenever the waveform level is high. In Figure 2.1 we show a typical sequence of binary NRZ data, and the resulting sequence of pits on the disk which result. The length of the shortest pit which can appear on the disc corresponds to the duration of one baud. In our analysis we assumed an inner disk radius of 7 centimeters, a disk rotational speed of 3 Hz, and a baud duration of $(4/3 \times 10^6)^{-1}$ seconds. One can readily determine that the corresponding minimum length of a pit on an inner track is $2\pi \times 7 \times 10^4 \times 3(\mu/\text{sec}) \times (4/3 \times 10^6)^{-1}$ sec = 0.99 microns. In our system simulation, we simplified the scattering geometry to one dimension; i.e., the waveform amplitude produced on playback is the convolution resulting from a one-dimensional beam intensity profile passing over a one-dimensional scattering pit. We furthermore assumed that the pit has uniform scattering properties along its entire length.

To arrive at a one-dimensional intensity profile for the reading beam, we assumed a perfectly circular, uniformly illuminated lens with a numerical aperture, N.A., of 0.63 and wavelength, $\lambda$, of 6328A. Under the assumption that the spot size of the focussed beam is limited only by diffraction, the resulting light amplitude at any point in the diffraction pattern is given by (ref. 1, sect. 6.8),

$$g(\alpha) = 2\pi a^2 J_1(\alpha)/\alpha,$$

where $J_1$ is the first order Bessel function, $a$ is the radius of the lens, $\alpha = 2\pi a \sin\theta/\lambda$, and $\theta$ is the angle subtended at the lens by any point in the diffraction pattern. In Figure 2.2 we have plotted $g^2(\alpha)$ normalized to unity. The radius, $\rho$, of the spot size (i.e., the distance from the center of the spot to the first null; $\alpha = 3.9$ in Figure 2.2) is given by (ref. 2, page 359)

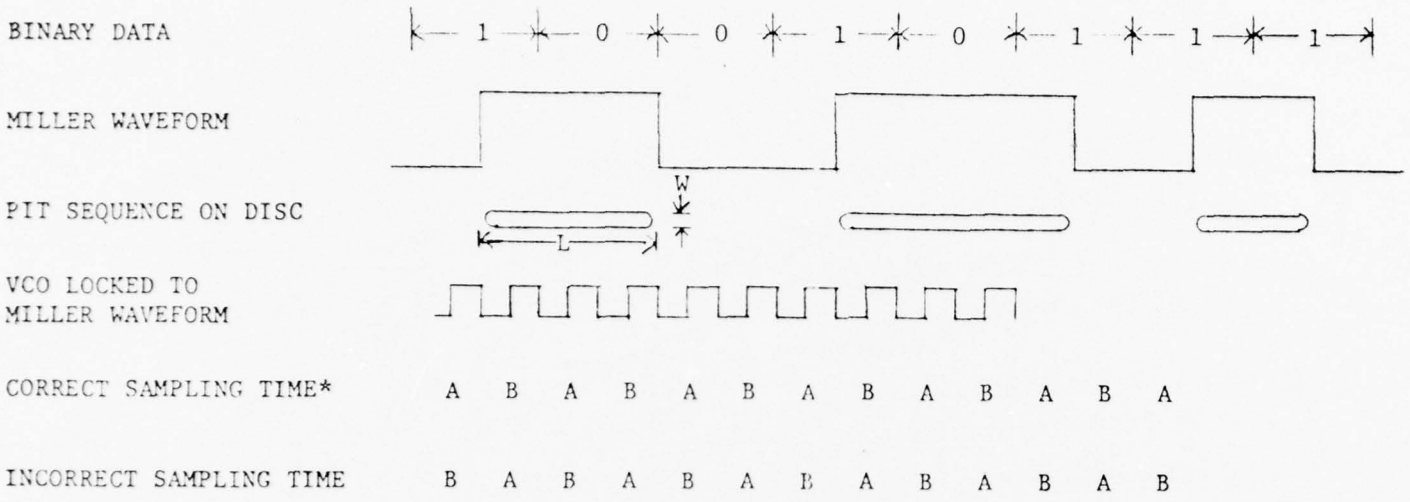


FIGURE 2.1

SOME ASPECTS OF MILLER MODULATION

*We assume that a pair of samples taken at time A and time B are used by the detector to estimate the original Binary Data.

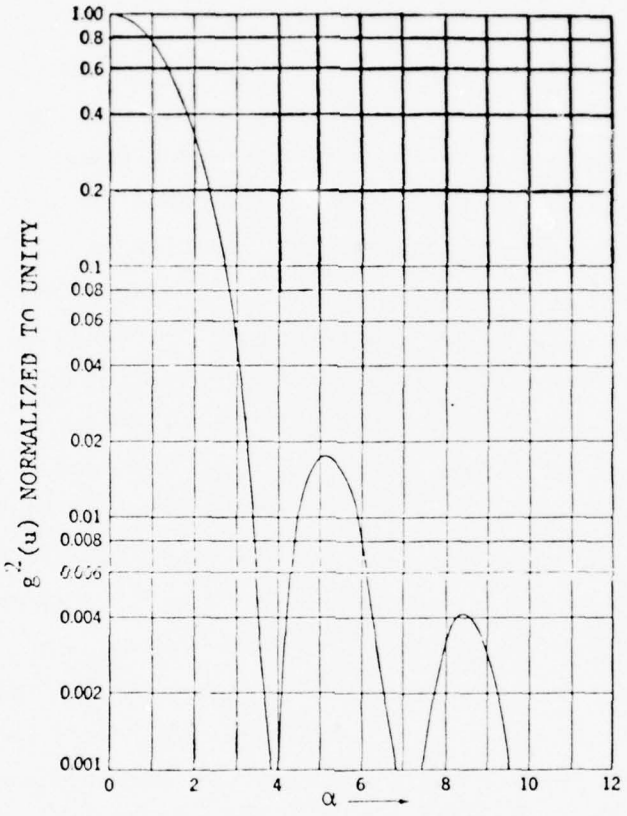


FIGURE 2.2

POWER PROFILE FOR DIFFRACTION PATTERN OF UNIFORMLY ILLUMINATED CIRCULAR LENS

$$\rho = 0.61\lambda/\text{N.A.}$$
$$= 0.61 \text{ microns}$$

In the system computer simulation, we used eight samples per baud to represent the waveform read from the disc. Since a baud occupies 0.99 microns while the beam is 1.22 microns from null to null, it is clear that samples of the beam amplitude taken from Figure 2.2 should be spaced by 0.79u. For expedience, however, we "eyeballed" points for the beam amplitude from Figure 2.2 at spacings of 1.0u. As a result, the beamwidth used in the simulation is about 20% more narrow than a numerical aperture of 0.63 would imply, and therefore the simulated performance will give results which are slightly better than might actually be expected.

It is "reassuring" to compare the frequency response of our simulated system with measured data provided by Bögels, *et al* (ref. 3). The frequency response for a video disc rotating at 30 Hz with a numerical aperture of 0.4, and an inner radius of 5.5 centimeters is given in Figure 12 of that reference. One can argue (see Appendix A) that the inverse Fourier transform of this frequency response represents the convolution of the read beam and the pit. This inverse transform appears plotted as the broken curve in Figure 2.3. The solid curve of Figure 2.3 is the convolution of the sampled beam amplitude used in the simulation with a 1 micron pit. (A "pit" is simulated by a sample value of 1, and a non-pit by a sample value of 0.) The similarity between the two curves of Figure 2.3 indicates that the frequency response of our simulated system is close to that indicated by Bögels. We also note that the symmetrical shape of the convolution shown in Figure 2.3 implies a linear phase response in the frequency domain.

FIGURE 2.3

Broken Curve: Inverse transform of video disc frequency response (ref. 3, fig. 12, d = 110 mm)

Solid Curve: Convolution of beam and pit used in analysis

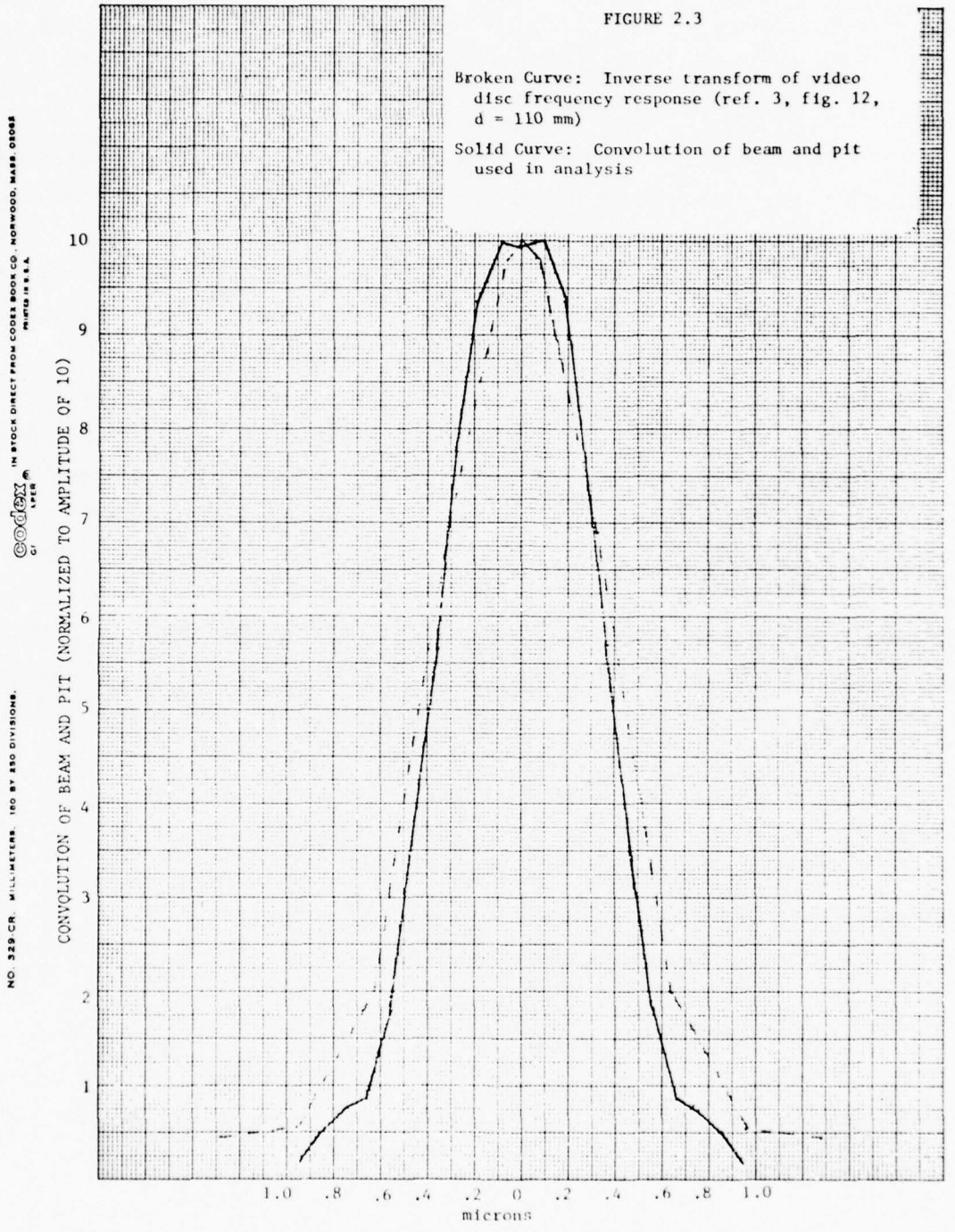

## 2.2 DATA RATE VARIATION DUE TO DISC ECCENTRICITY AND ITS EFFECT ON PLL DESIGN.

In order to provide a data clock to the user as well as provide timing for the demodulation circuitry, it will be necessary to phase lock a voltage-controlled oscillator to the waveform read from the disc. The phase locked loop (PLL) must be capable of remaining locked even when the data rate read from the disk differs from its nominal value. The extent of this rate difference is determined by the eccentricity of the disc. A maximum value of $\pm 50$ microns of eccentricity has been assumed in our design analysis. If the radius is 7 centimeters, a $\pm 50$ micron eccentricity will result in a change in data rate of $\pm 50$ parts in $7 \times 10^4$. Consequently, if the data rate is nominally 4/3 MHz, we can expect a rate offset as large as $\pm 952$ Hz (say, 1 kHz for round numbers).

In order to design the PLL, we must determine how accurately we wish to maintain lock. This, in turn, is a function of how much phase error can be tolerated by the data detection circuitry (and still result in error-free data!). For this answer we anticipate the results of Section 4 in which we determined that the data detector is capable of operating (error-free) over a phase margin of about $\pm 60$ degrees (one baud corresponds to 360 degrees). We will design our PLL so that, with a 1000 Hz offset, the phase error is no more than $\pm 10$ degrees (i.e., about 20% of the allowable margin). From reference 4 (equation 4-4a, page 29), the relation between the phase error, frequency offset and loop gain of a second order PLL is given by

$$\theta = \Delta\omega / K$$

where K is the loop gain, $\Delta\omega$ is the frequency offset (radians/sec) and $\theta$ is the phase error (radians). Consequently, to provide a phase error of only 10 degrees with a 1 kHz frequency offset requires a loop gain, K, of 36000.

In addition to the loop gain, K, we must specify the loop bandwidth, $\omega_n$, and damping factor, $\xi$, to complete specify the second order loop design. In our analysis we have used a value of $\xi = 0.707$ (to minimize both transient response and loop noise bandwidth) and a value

of $\omega_n$ determined by the desire to acquire phase lock reasonably quickly. We will define "reasonably quickly" to be a phase error of no more than 10% after 200 bit times. In reference 4 (page 34) it is shown that the residual phase error has decreased to 10% of its original value after a period of time given by $\omega_n t = 3.6$ ($\xi = 0.707$). Since 200 bit times corresponds to 150 microseconds, we have

$$\text{Loop Bandwidth} = \frac{3.6}{2\pi \cdot 150 \cdot 10^{-6}} = 3.8 \times 10^3$$

We note that correct data will appear at the output of the detector in considerably less than 200 bit times. In particular, correct data will be demodulated with a phase error as large as 60 degrees. Since the initial phase error can be no worse than $180^o$, the phase error is less than 33% ($60^o$) in about 40 bit times.

## 3.0 MODELLING OF DEMODULATOR OPERATIONS

Because the Miller waveform is distorted by the filtering operations described previously, the following two questions required answers:

1) Is there a detector design which, *when properly synchronized to baud timing*, can process the distorted waveform to provide error-free demodulated data?
2) Will the phase locked loop work well enough on the distorted waveform to provide reliable baud timing to the detector?

A Monte Carlo simulation of the system was written (in FORTRAN) to obtain answers to these questions. A block diagram of the system is given in Figure 3.1, and the program listing is given in Appendix B. The dotted lines of Figure 3.1 indicate the various system parameters which were made easily changeable in the program. The FORTRAN names of each of these parameters appear on the figure.

### 3.1 DETECTOR DESIGN

Several types of detector designs were tested to determine their comparative performance under the assumption that *perfect* baud timing was available to the detector. The simplest type of detector tested was one which simply compared the signs of the sample taken in the middle of the first half, and middle of the second half of a baud. If the signs were the same, a logic 0 decision is made, and a 1 decision otherwise. From Figure 2.1 we observe that this detector will give error-free performance if the waveform is undistorted.

Figure 3.2 shows the sampled data waveform from several consecutive bauds of the distorted Miller waveform. The simple detector just described would compare the sign of S3 and S7 to make a binary decision.* The simulation is set up in such a fashion that an error count can be made for *all eight* possible starting points of the detector. If at least one of these starting points consistently gives error-free performance, we may conclude that the detector will work satisfactorily (if the PLL can provide it with a proper baud clock, of course).

*In the simulation the baud boundary is known perfectly, of course, and contains eight consecutive samples of the distorted waveform S1, S2,...,S8 (see Figure 3.2).

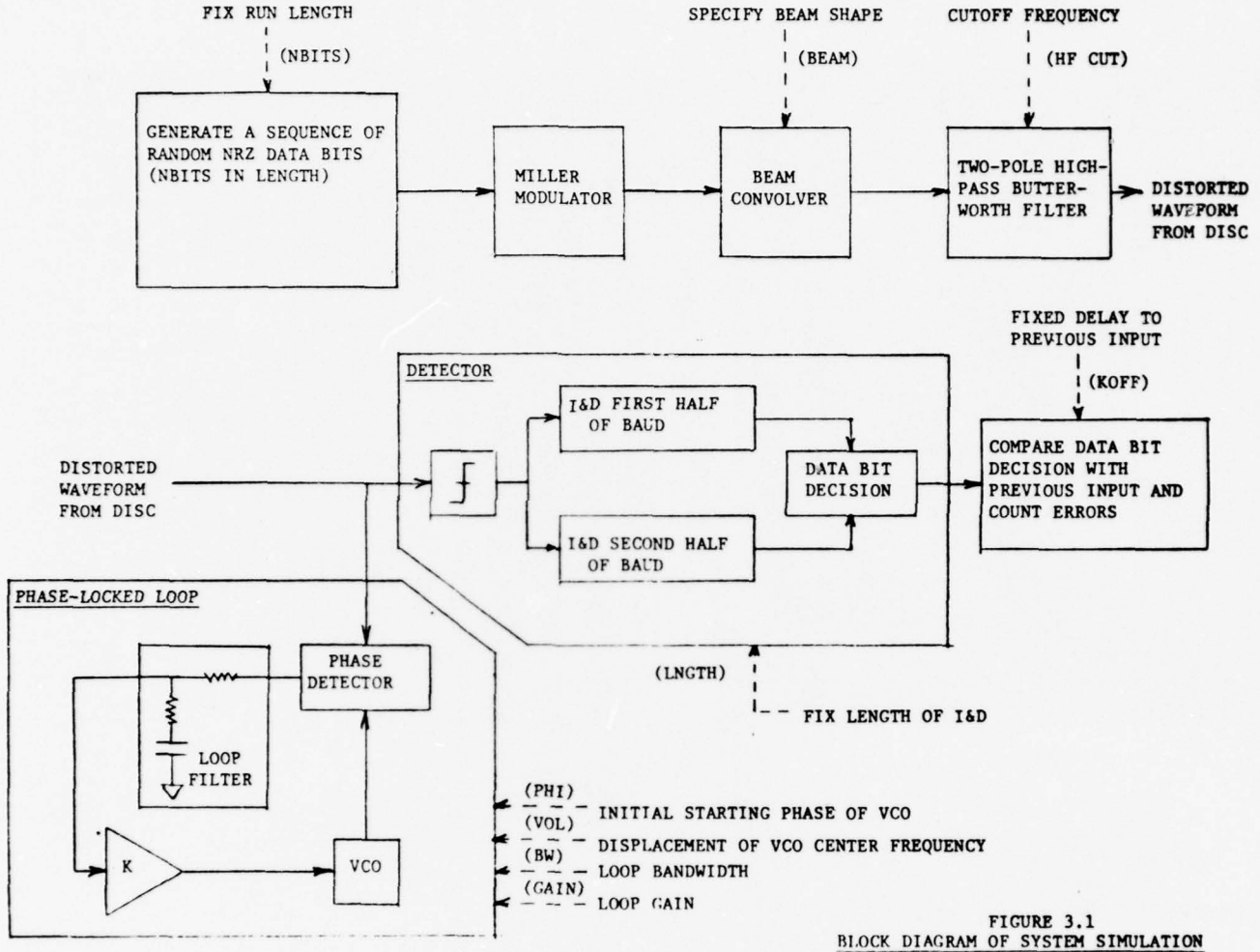


FIGURE 3.1
BLOCK DIAGRAM OF SYSTEM SIMULATION

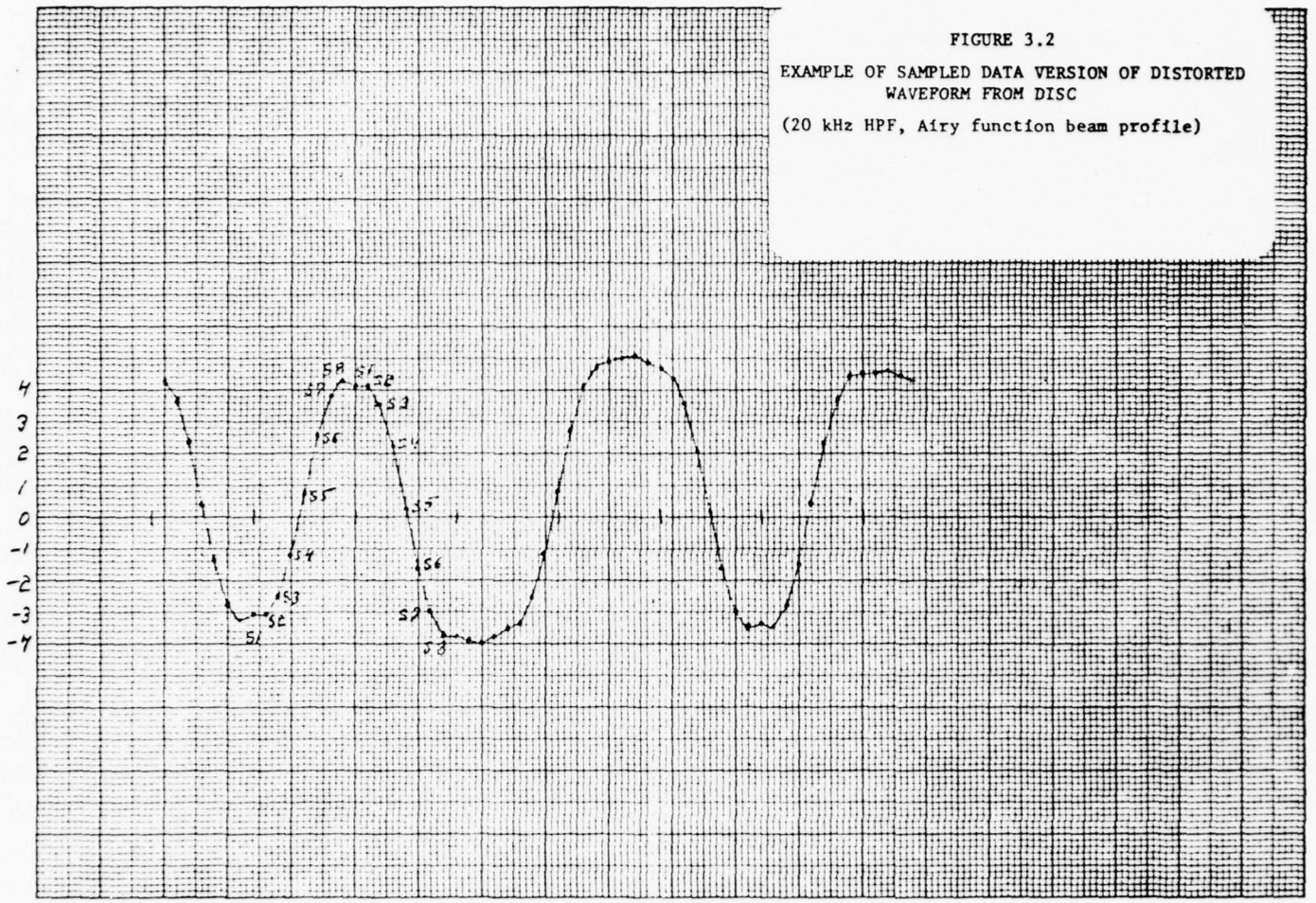


FIGURE 3.2

EXAMPLE OF SAMPLED DATA VERSION OF DISTORTED WAVEFORM FROM DISC

(20 kHz HPF, Airy function beam profile)

A detector for which several consecutive starting points give error-free detection is clearly better than one for which only a single error-free starting point exists, since such a detector would be more tolerant of timing error from the phase locked loop. The number of error-free starting points provides us with a means for comparing detector designs. We note in passing that if the waveform were distortion-free, the maximum of four consecutive error-free starting points would be found.

For a 20 kHz highpass laser beam filter, this simple detector was found to work quite well. For higher cutoff frequencies, however, a slightly modified detector design was required. This detector formed

$$A = \text{sign}[\text{sign}(S1)+\text{sign}(S2)+\text{sign}(S3)]$$

and

$$B = \text{sign}[\text{sign}(S5)+\text{sign}(S6)+\text{sign}(S7)],$$

and made a logic 0 decision if A and B had the same sign (1 otherwise). Again, all eight possible starting points are considered in the program (i.e., the value of A for the second starting point is given by sign[sign(S2)+sign(S3)+sign(S4)], etc.) and, in addition, the number of consecutive points within the brackets could be varied by the parameter LNGTH in the FORTRAN program. A value of LNGTH = 3 gave consistently best results for all cutoff frequencies.

An analog integrate-and-dump detector was also tried, i.e., A = sign[S1+S2+S3], B = sign[S5+S6+S7], and found to give consistently poorer results than the hardlimiting detector just described.

## 3.2 PHASE LOCKED LOOP SIMULATION

In the PLL simulation, we built a linear phase detector by the simple expeident of using a VCO with a "sawtooth" output shown in Figure 3.3 below, where $T = ((8/3)\ \text{MHz})^{-1}$. The value of the VCO

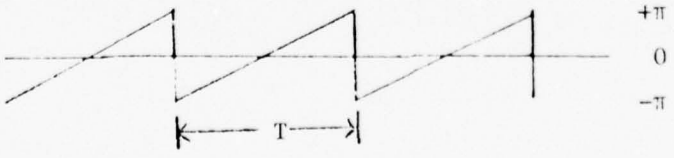


FIGURE 3.3

VCO OUTPUT

sawtooth is sampled at the time of a zero crossing in the distorted waveform, and appears at the input to the loop filter until the next zero crossing.*

The ability to introduce a frequency offset to test performance with disc eccentricity was included in the program. As far as the PLL is concerned, there is no difference between a frequency offset on the data coming from the disc, or an offset in the VCO center frequency. The latter was much easier to program. A worst-case test was set up in which the operator could introduce a fixed frequency offset (of arbitrary size) at any arbitrary time (determined by a switch position on the computer).

*Since only a sampled data version of the distorted waveform is available, the location of the zero crossing is determined by a linear extrapolation between the two samples of differing signs.

## 4.0 SIMULATION RESULTS

The simulation results indicate that the demodulator and PLL described in the previous sections will provide excellent performance for the distortion conditions simulated. This is evident from the simulation printout shown in Figure 4.1. This printout begins with a summary of all the system parameters shown in Figure 3.1, including the sampled amplitude of the read beam. This is followed by twelve columns which contain the following information:

Column #1: How far the run has progressed; i.e., the data baud number (results are printed out only on every tenth data baud).

Column #2: The sample number of the *first* time in the baud when the VCO flips from $+\pi$ to $-\pi$.

Column #3: The sample number (extrapolated to two decimal points) of the most recent zero crossing in the distorted waveform *prior* to the VCO flip time recorded in Column 2. Note that a number greater than 4 in this column corresponds to a zero crossing in the previous baud. Note also that zero crossings in the distorted waveform tend to occur at two different points within a baud (about 7.75 and 3.75) as expected for Miller modulation.

Column #4: The same information as given in Column 2 except that the VCO flip time (i.e., sample number) is extrapolated to two decimal places.

Columns #5-#12: Accumulated number of detector errors corresponding to each of the eight possible starting points for the detector.

We observe the following performance characteristics from Figure 4.1. First, we note that three consecutive detector positions (out of a maximum of four) give error-free performance. Secondly, from Column 4, we observe that the phase jitter on the VCO, after the initial locking transient has decayed (somewhere about 80 to 90 baud times), has a peak-to-peak variation of only about 0.2 of a sample interval. Since the margin for detector timing error is so much larger than this (three

NUMBER OF TEST BITS 1000 HF CUT OFF, IN KHZ 20.0000 # SMPS. IN INT 3

PL. GAIN 36000. PLL BW 5300. INITIAL VCOPHASE(DEG) 135.

VALUE OF KOFF 3

DISPLACMENT FROM VCO TO DET. 0

DOPP OFFSET IN HZ (SW#7) 1000. DOPP RATE IN HZ/ SEC(SW#8) 0.

SAMPLED AMPLITUDE OF THE READ BEAM

| | | | | | | | | | | | |
|---|---|---|---|---|---|---|---|---|---|---|---|
| 0.000 | 0.000 | 0.000 | 0.000 | 0.000 | 0.000 | 0.000 | 0.000 | | | | |
| 0.000 | 0.000 | 0.000 | 0.000 | 0.000 | 0.000 | 0.000 | 0.000 | | | | |
| 0.000 | 0.000 | 0.000 | 0.000 | 0.030 | 0.050 | 0.130 | 0.110 | | | | |
| 0.060 | 0.410 | 0.710 | 0.960 | 0.960 | 0.710 | 0.410 | 0.060 | | | | |
| 0.110 | 0.130 | 0.050 | 0.030 | 0.000 | 0.000 | 0.000 | 0.000 | | | | |
| 0.000 | 0.000 | 0.000 | 0.000 | 0.000 | 0.000 | 0.000 | 0.000 | | | | |
| 0.000 | 0.000 | 0.000 | 0.000 | 0.000 | 0.000 | 0.000 | 0.000 | | | | |
| 1 | 3 | 0.00 | 3.50 | 0 | 0. | 0. | 0. | 0. | 0. | 0. | 0. |
| 11 | 3 | 3.90 | 3.59 | 7. | 0. | 0. | 0. | 0. | 7. | 7. | 7. |
| 21 | 3 | 7.87 | 3.71 | 15. | 3. | 0. | 0. | 0. | 11. | 14. | 14. |
| 31 | 3 | 7.60 | 3.89 | 21. | 3. | 0. | 0. | 0. | 17. | 20. | 20. |
| 41 | 4 | 7.62 | 4.10 | 29. | 7. | 0. | 0. | 0. | 21. | 28. | 28. |
| 51 | 4 | 7.89 | 4.36 | 37. | 10. | 0. | 0. | 0. | 26. | 36. | 36. |
| 61 | 4 | 0.57 | 4.55 | 44. | 12. | 0. | 0. | 0. | 31. | 43. | 43. |
| 71 | 4 | 7.88 | 4.77 | 52. | 14. | 0. | 0. | 0. | 37. | 51. | 51. |
| 81 | 4 | 3.76 | 4.89 | 58. | 15. | 0. | 0. | 0. | 43. | 58. | 58. |
| 91 | 4 | 7.86 | 4.95 | 67. | 16. | 0. | 0. | 0. | 50. | 66. | 66. |
| 101 | 4 | 7.91 | 4.94 | 76. | 16. | 0. | 0. | 0. | 59. | 75. | 75. |
| 111 | 4 | 0.02 | 4.82 | 82. | 17. | 0. | 0. | 0. | 64. | 81. | 81. |
| 121 | 4 | 7.96 | 4.83 | 89. | 20. | 0. | 0. | 0. | 68. | 88. | 88. |
| 131 | 4 | 7.67 | 4.84 | 96. | 22. | 0. | 0. | 0. | 73. | 95. | 95. |
| 141 | 4 | 3.56 | 4.77 | 103. | 25. | 0. | 0. | 0. | 78. | 103. | 103. |
| 151 | 4 | 3.49 | 4.75 | 111. | 29. | 0. | 0. | 0. | 82. | 111. | 111. |
| 161 | 4 | 3.79 | 4.76 | 119. | 33. | 0. | 0. | 0. | 86. | 119. | 119. |
| 171 | 4 | 3.92 | 4.92 | 128. | 33. | 0. | 0. | 0. | 95. | 128. | 128. |
| 181 | 4 | 7.93 | 4.93 | 137. | 35. | 0. | 0. | 0. | 101. | 136. | 136. |
| 191 | 4 | 7.75 | 4.84 | 143. | 36. | 0. | 0. | 0. | 106. | 142. | 142. |
| 201 | 4 | 3.68 | 4.83 | 151. | 36. | 0. | 0. | 0. | 114. | 150. | 150. |
| 211 | 4 | 3.81 | 4.81 | 158. | 38. | 0. | 0. | 0. | 120. | 158. | 158. |
| 221 | 4 | 7.63 | 4.81 | 167. | 38. | 0. | 0. | 0. | 128. | 166. | 166. |
| 231 | 4 | 7.83 | 4.82 | 175. | 39. | 0. | 0. | 0. | 135. | 174. | 174. |
| 241 | 4 | 7.76 | 4.86 | 183. | 41. | 0. | 0. | 0. | 141. | 182. | 182. |
| 251 | 4 | 0.03 | 4.89 | 191. | 42. | 0. | 0. | 0. | 148. | 190. | 190. |
| 261 | 4 | 3.98 | 4.92 | 199. | 46. | 0. | 0. | 0. | 153. | 199. | 199. |
| 271 | 4 | 3.94 | 4.93 | 206. | 46. | 0. | 0. | 0. | 160. | 206. | 206. |
| 281 | 4 | 7.67 | 4.83 | 213. | 47. | 0. | 0. | 0. | 165. | 212. | 212. |
| 291 | 4 | 7.70 | 4.79 | 219. | 47. | 0. | 0. | 0. | 171. | 218. | 218. |
| 301 | 4 | 7.74 | 4.74 | 226. | 48. | 0. | 0. | 0. | 177. | 225. | 225. |
| 311 | 4 | 3.40 | 4.81 | 233. | 51. | 0. | 0. | 0. | 182. | 233. | 233. |
| 321 | 4 | 3.95 | 4.80 | 241. | 53. | 0. | 0. | 0. | 187. | 240. | 240. |
| 331 | 4 | 7.48 | 4.82 | 248. | 56. | 0. | 0. | 0. | 191. | 247. | 247. |
| 341 | 4 | 7.89 | 4.87 | 256. | 57. | 0. | 0. | 0. | 198. | 255. | 255. |
| 351 | 4 | 4.11 | 4.90 | 261. | 59. | 0. | 0. | 0. | 201. | 261. | 261. |

REQ. STEP STARTS HERE

| | | | | | | | | | | | |
|---|---|---|---|---|---|---|---|---|---|---|---|
| 361 | 4 | 0.04 | 4.84 | 269. | 63. | 0. | 0. | 0. | 205. | 268. | 268. |
| 371 | 4 | 0.57 | 4.84 | 276. | 66. | 0. | 0. | 0. | 209. | 275. | 275. |
| 381 | 4 | 7.81 | 4.83 | 283. | 70. | 0. | 0. | 0. | 212. | 282. | 282. |

FIGURE 4.1

SIMULATION RESULTS FOR TYPICAL SYSTEM PARAMETERS

| | | | | | | | | | | | |
|---|---|---|---|---|---|---|---|---|---|---|---|
| 241 | 4 | 7.76 | 4.86 | 183. | 41. | 0. | 0. | 0. | 141. | 182. | 182. |
| 251 | 4 | 0.03 | 4.89 | 191. | 42. | 0. | 0. | 0. | 148. | 190. | 190. |
| 261 | 4 | 3.98 | 4.92 | 199. | 46. | 0. | 0. | 0. | 153. | 199. | 199. |
| 271 | 4 | 3.94 | 4.93 | 206. | 46. | 0. | 0. | 0. | 160. | 206. | 206. |
| 281 | 4 | 7.67 | 4.83 | 213. | 47. | 0. | 0. | 0. | 165. | 212. | 212. |
| 291 | 4 | 7.70 | 4.79 | 219. | 47. | 0. | 0. | 0. | 171. | 218. | 218. |
| 301 | 4 | 7.74 | 4.74 | 226. | 48. | 0. | 0. | 0. | 177. | 225. | 225. |
| 311 | 4 | 3.40 | 4.81 | 233. | 51. | 0. | 0. | 0. | 182. | 233. | 233. |
| 321 | 4 | 3.95 | 4.80 | 241. | 53. | 0. | 0. | 0. | 187. | 240. | 240. |
| 331 | 4 | 7.48 | 4.82 | 248. | 56. | 0. | 0. | 0. | 191. | 247. | 247. |
| 341 | 4 | 7.89 | 4.87 | 256. | 57. | 0. | 0. | 0. | 198. | 255. | 255. |
| 351 | 4 | 4.11 | 4.90 | 261. | 59. | 0. | 0. | 0. | 201. | 261. | 261. |
| FREQ. STEP STARTS HERE | | | | | | | | | | | |
| 361 | 4 | 0.04 | 4.84 | 269. | 63. | 0. | 0. | 0. | 205. | 268. | 268. |
| 371 | 4 | 0.57 | 4.84 | 276. | 66. | 0. | 0. | 0. | 209. | 275. | 275. |
| 381 | 4 | 7.81 | 4.83 | 283. | 70. | 0. | 0. | 0. | 212. | 282. | 282. |
| 391 | 4 | 7.61 | 4.81 | 290. | 72. | 0. | 0. | 0. | 217. | 289. | 289. |
| 401 | 4 | 7.85 | 4.82 | 297. | 73. | 0. | 0. | 0. | 223. | 296. | 296. |
| 411 | 4 | 0.08 | 4.85 | 304. | 75. | 0. | 0. | 0. | 228. | 303. | 303. |
| 421 | 4 | 3.97 | 4.81 | 311. | 78. | 0. | 0. | 0. | 233. | 311. | 311. |
| 431 | 4 | 7.59 | 4.76 | 319. | 81. | 0. | 0. | 0. | 237. | 318. | 318. |
| 441 | 4 | 7.73 | 4.79 | 326. | 82. | 0. | 0. | 0. | 243. | 325. | 325. |
| 451 | 4 | 3.42 | 4.86 | 334. | 84. | 0. | 0. | 0. | 249. | 333. | 333. |
| 461 | 4 | 3.49 | 4.85 | 342. | 88. | 0. | 0. | 0. | 253. | 341. | 341. |
| 471 | 4 | 0.06 | 4.82 | 349. | 91. | 0. | 0. | 0. | 257. | 348. | 348. |
| 481 | 4 | 3.95 | 4.79 | 357. | 93. | 0. | 0. | 0. | 263. | 356. | 356. |
| 491 | 4 | 7.86 | 4.86 | 366. | 94 | 0. | 0. | 0. | 271. | 365. | 365. |
| 501 | 4 | 7.77 | 4.86 | 373. | 95. | 0. | 0. | 0. | 277. | 372. | 372. |
| 511 | 4 | 0.07 | 4.86 | 381. | 96. | 0. | 0. | 0. | 284. | 380. | 380. |
| 521 | 4 | 3.78 | 4.86 | 389. | 99. | 0. | 0. | 0. | 290. | 389. | 389. |
| 531 | 4 | 7.97 | 4.87 | 397. | 100. | 0. | 0. | 0. | 296. | 396. | 396. |
| 541 | 4 | 4.00 | 4.86 | 404. | 101. | 0. | 0. | 0. | 303. | 404. | 404. |
| 551 | 4 | 3.91 | 4.77 | 411. | 101. | 0. | 0. | 0. | 310. | 411. | 411. |
| 561 | 4 | 0.05 | 4.76 | 419. | 102. | 0. | 0. | 0. | 316. | 418. | 418. |
| 571 | 4 | 3.51 | 4.71 | 425. | 104. | 0. | 0. | 0. | 321. | 425. | 425. |
| 581 | 4 | 7.39 | 4.77 | 433. | 107. | 0. | 0. | 0. | 325. | 432. | 432. |
| 591 | 4 | 7.87 | 4.75 | 439. | 109. | 0. | 0. | 0. | 329. | 438. | 438. |
| 601 | 4 | 7.78 | 4.76 | 445. | 109. | 0. | 0. | 0. | 335. | 444. | 444. |
| 611 | 4 | 7.79 | 4.80 | 453. | 112. | 0. | 0. | 0. | 340. | 452. | 452. |
| 621 | 4 | 7.96 | 4.90 | 463. | 113. | 0. | 0. | 0. | 349. | 462. | 462. |
| 631 | 4 | 4.20 | 4.91 | 470. | 116. | 0. | 0. | 0. | 353. | 470. | 470. |
| 641 | 4 | 3.90 | 4.89 | 478. | 119. | 0. | 0. | 0. | 358. | 477. | 477. |
| 651 | 4 | 7.93 | 4.88 | 485. | 120. | 0. | 0. | 0. | 364. | 484. | 484. |
| 661 | 4 | 3.51 | 4.93 | 493. | 122. | 0. | 0. | 0. | 370. | 492. | 492. |
| 671 | 4 | 7.89 | 4.92 | 501. | 125. | 0. | 0. | 0. | 375. | 500. | 500. |
| 681 | 4 | 0.33 | 4.79 | 507. | 126. | 0. | 0. | 0. | 380. | 506. | 506. |

FIGURE 4.1
(Concluded)

consecutive sample intervals!), it is clear that detection timing referenced to the VCO zero crossings will give error-free performance with a wide margin to spare.

Next, we observe that a 1000 Hz frequency (doppler) *step* is introduced at the 361-st baud. As already noted, this is a considerably more severe frequency offset profile than will result from normal disc eccentricity. The resulting shift in the VCO zero crossing position, however, is observed to be insignificantly small compared to the detector time error margin.

Figure 4.2 is the same as Figure 4.1 except that the starting phase of the VCO was shifted from 135 to 225 degrees. The initial transient time is observed to be somewhat longer (about 100 bauds, which is the maximum observed). Since the VCO phase jitter is so small (compared to the allowable margin), it is clear that a wider loop bandwidth (PLL BW) can be used to shorten transient time.

It is interesting to observe the effect of the laser noise highpass filter cutoff frequency on demodulator performance. Figures 4.3, 4.4 and 4.5 correspond to identical conditions as Figure 4.1 except that the filter cutoff is respectively, 75, 150 and 225 kHz.* Decreasing detector margin and increasing variation in the VCO phase reference is observed with increasing cutoff frequency. The simulations indicate that a 100 kHz highpass filter is about the upper limit at which adequate demodulation can be achieved. Note that as the HPF cutoff frequency increases, not only does the detection margin decrease, but also the detector "start" time changes (relative to the VCO phase). A retiming single-shot is provided in the hardware for this reason (see Section 5).

It is interesting to determine the sensitivity of system performance to various profiles of the read beam. To get a feeling for this, a sampled beam amplitude profile of (1,1,1,1,1,1,1,1) was tested, and the results appear in Figure 4.6. We observe that clock extraction is still

*The starting phase in Figures 4.3, 4.4 and 4.5 was selected to be $45^{o}$ but this is an insignificant parameter change.

very accurate, however, detector phase margin is reduced to about $\pm 22\text{-}1/2$ degrees. In general, we may conclude that system performance is reasonably insensitive to modest changes in the beam profile.

NUMBER OF TEST BITS 1000 HF CUT OFF, IN KHZ 20.0000 # SMPS. IN INT 3

PLL GAIN 36000. PLL BW 5300. INITIAL VCOPHASE(DEG) 225.

VALUE OF KOFF 3

DISPLACMENT FROM VCO TO DET. 0

DOPP OFFSET IN HZ (SW#7) 1000. DOPP RATE IN HZ/ SEC(SW#8) 0.

SAMPLED AMPLITUDE OF THE READ BEAM

| | | | | | | | | | | | |
|---|---|---|---|---|---|---|---|---|---|---|---|
| 0.000 | 0.000 | 0.000 | 0.000 | 0.000 | 0.000 | 0.000 | 0.000 | | | | |
| 0.000 | 0.000 | 0.000 | 0.000 | 0.000 | 0.000 | 0.000 | 0.000 | | | | |
| 0.000 | 0.000 | 0.000 | 0.000 | 0.030 | 0.050 | 0.130 | 0.110 | | | | |
| 0.060 | 0.410 | 0.710 | 0.960 | 0.960 | 0.710 | 0.410 | 0.060 | | | | |
| 0.110 | 0.130 | 0.050 | 0.030 | 0.000 | 0.000 | 0.000 | 0.000 | | | | |
| 0.000 | 0.000 | 0.000 | 0.000 | 0.000 | 0.000 | 0.000 | 0.000 | | | | |
| 0.000 | 0.000 | 0.000 | 0.000 | 0.000 | 0.000 | 0.000 | 0.000 | | | | |
| 1 | 2 | 0.00 | 2.50 | 0. | 0. | 0. | 0 | 0. | 0. | 0 | 0 |
| 11 | 2 | 3.90 | 2.44 | 7. | 0. | 0. | 0. | 0. | 7. | 7. | 7. |
| 21 | 2 | 7.87 | 2.37 | 15. | 3. | 0. | 0. | 0. | 11. | 14. | 14. |
| 31 | 2 | 7.60 | 2.29 | 21. | 3. | 0. | 0. | 0. | 17. | 20 | 20. |
| 41 | 2 | 7.62 | 2.17 | 29. | 7. | 0. | 0. | 0. | 21. | 28 | 28. |
| 51 | 2 | 7.89 | 2.03 | 37. | 10. | 0 | 0. | 0. | 26. | 36. | 36. |
| 61 | 1 | 0.57 | 1.86 | 44. | 12. | 0. | 0. | 0. | 31. | 43. | 43. |
| 71 | 1 | 7.88 | 1.65 | 52. | 14. | 0. | 0. | 0. | 37. | 51. | 51. |
| 81 | 1 | 3.76 | 1.40 | 58. | 15. | 0. | 0. | 0. | 43. | 58. | 58. |
| 91 | 1 | 7.86 | 1.08 | 67. | 16. | 0. | 0. | 0. | 50. | 66. | 66. |
| 101 | 4 | 7.91 | 4.92 | 76. | 16. | 0. | 0. | 0. | 59. | 75. | 75. |
| 111 | 4 | 0.02 | 4.71 | 82. | 17. | 0. | 0. | 0. | 64. | 81. | 81. |
| 121 | 4 | 7.96 | 4.60 | 89. | 20. | 0. | 0. | 0. | 68. | 88. | 88. |
| 131 | 4 | 7.67 | 4.64 | 96. | 22. | 0. | 0. | 0. | 73. | 95. | 95. |
| 141 | 4 | 3.56 | 4.71 | 103. | 25. | 0. | 0 | 0. | 78. | 103. | 103. |
| 151 | 4 | 3.49 | 4.68 | 111. | 29. | 0. | 0. | 0. | 82. | 111. | 111. |
| 161 | 4 | 3.79 | 4.68 | 119. | 33. | 0. | 0. | 0. | 86. | 119. | 119. |
| 171 | 4 | 3.92 | 4.92 | 128. | 33. | 0 | 0. | 0. | 95. | 128. | 128. |
| 181 | 4 | 7.93 | 4.90 | 137. | 35. | 0. | 0 | 0. | 101. | 136. | 136. |
| 191 | 4 | 7.75 | 4.81 | 143. | 36. | 0. | 0. | 0. | 106. | 142. | 142. |
| 201 | 4 | 3.68 | 4.88 | 151. | 36. | 0. | 0. | 0. | 114. | 150. | 150. |
| 211 | 4 | 3.81 | 4.80 | 158. | 38. | 0. | 0. | 0. | 120. | 158. | 158. |
| 221 | 4 | 7.63 | 4.81 | 167. | 38. | 0. | 0. | 0. | 128. | 166. | 166. |
| 231 | 4 | 7.83 | 4.84 | 175. | 39. | 0. | 0. | 0. | 135. | 174. | 174. |
| 241 | 4 | 7.76 | 4.88 | 183. | 41. | 0. | 0 | 0. | 141. | 182. | 182. |
| 251 | 4 | 0.03 | 4.92 | 191. | 42. | 0. | 0. | 0. | 148. | 190. | 190. |
| 261 | 4 | 3.98 | 4.95 | 199. | 46. | 0. | 0. | 0. | 153. | 199. | 199. |
| 271 | 4 | 3.94 | 4.89 | 206. | 46. | 0. | 0. | 0. | 160. | 206. | 206. |

FIGURE 4.2

VCO LOCK TIME CHANGES WITH DIFFERENT INITIAL VCO PHASE

NUMBER OF TEST BITS 1000 HF CUT OFF, IN KHZ 75.0000 # SMPS. IN INT 3

LL GAIN 36000. PLL BW 5300. INITIAL VCOPHASE(DEG) 45.

VALUE OF KOFF 3

DISPLACMENT FROM VCO TO DET. 0

OPP OFFSET IN HZ (SW#7) 1000. DOPP RATE IN HZ/ SEC(SW#8) 0.

SAMPLED AMPLITUDE OF THE READ BEAM

| | | | | | | | | | | | |
|---|---|---|---|---|---|---|---|---|---|---|---|
| 0.000 | 0.000 | 0.000 | 0.000 | 0.000 | 0.000 | 0.000 | 0.000 | 0.000 | 0.000 | 0.000 | |
| 0.000 | 0.000 | 0.000 | 0.000 | 0.000 | 0.000 | 0.000 | 0.000 | 0.000 | 0.000 | 0.000 | |
| 0.000 | 0.000 | 0.000 | 0.000 | 0.030 | 0.050 | 0.130 | 0.110 | | | | |
| 0.060 | 0.410 | 0.710 | 0.960 | 0.960 | 0.710 | 0.410 | 0.060 | | | | |
| 0.110 | 0.130 | 0.050 | 0.030 | 0.000 | 0.000 | 0.000 | 0.000 | | | | |
| 0.000 | 0.000 | 0.000 | 0.000 | 0.000 | 0.000 | 0.000 | 0.000 | | | | |
| 0.000 | 0.000 | 0.000 | 0.000 | 0.000 | 0.000 | 0.000 | 0.000 | | | | |
| 1 | 4 | 3.73 | 4.50 | 0. | 0. | 0. | 0. | 0. | 0. | 0. | 0. |
| 11 | 4 | 3.66 | 4.67 | 7. | 0. | 0. | 0. | 0. | 7. | 7. | 7. |
| 21 | 4 | 6.81 | 4.69 | 14. | 3. | 0. | 0. | 1. | 11. | 14. | 14. |
| 31 | 4 | 6.97 | 4.61 | 18. | 4. | 0. | 0. | 3. | 16. | 20. | 20. |
| 41 | 4 | 7.88 | 4.61 | 23. | 6. | 0. | 0. | 6. | 22. | 28. | 28. |
| 51 | 4 | 7.90 | 4.46 | 31. | 6. | 0. | 0. | 6. | 30. | 36. | 36. |
| 61 | 4 | 0.40 | 4.50 | 35. | 8. | 0. | 0. | 9. | 35. | 43. | 43. |
| 71 | 4 | 7.59 | 4.50 | 41. | 10. | 0. | 0. | 11. | 41. | 51. | 51. |
| 81 | 4 | 3.58 | 4.43 | 45. | 11. | 0. | 0. | 13. | 47. | 58. | 58. |
| 91 | 4 | 7.65 | 4.45 | 53. | 12. | 0. | 0. | 14. | 54. | 66. | 66. |
| 101 | 4 | 7.77 | 4.52 | 62. | 12. | 0. | 0. | 14. | 63. | 75. | 75. |
| 111 | 4 | 0.20 | 4.40 | 65. | 13. | 0. | 0. | 17. | 68. | 81. | 81. |
| 121 | 4 | 0.34 | 4.33 | 69. | 15. | 0. | 0. | 20. | 73. | 88. | 88. |
| 131 | 4 | 7.28 | 4.31 | 74. | 17. | 0. | 0. | 22. | 78. | 95. | 95. |
| 141 | 4 | 2.62 | 4.31 | 79. | 18. | 0. | 0. | 25. | 85. | 103. | 103. |
| 151 | 4 | 3.20 | 4.40 | 85. | 19. | 0. | 0. | 26. | 92. | 111. | 111. |
| 161 | 4 | 3.87 | 4.44 | 93. | 19. | 0. | 0. | 26. | 100. | 119. | 119. |
| 171 | 4 | 3.64 | 4.62 | 101. | 19. | 0. | 0. | 27. | 109. | 128. | 128. |
| 181 | 4 | 7.23 | 4.68 | 109. | 21. | 0. | 0. | 28. | 115. | 136. | 136. |
| 191 | 4 | 7.28 | 4.55 | 113. | 22. | 0. | 0. | 30. | 120. | 142. | 142. |
| 201 | 4 | 2.92 | 4.47 | 121. | 22. | 0. | 0. | 30. | 128. | 150. | 150. |
| 211 | 4 | 3.78 | 4.51 | 126. | 23. | 0. | 0. | 32. | 135. | 158. | 158. |
| 221 | 4 | 3.74 | 4.59 | 133. | 24. | 0. | 0. | 34. | 142. | 166. | 166. |
| 231 | 4 | 7.52 | 4.58 | 141. | 25. | 0. | 0. | 34. | 149. | 174. | 174. |
| 241 | 4 | 6.86 | 4.51 | 148. | 27. | 0. | 0. | 35. | 155. | 182. | 182. |
| 251 | 4 | 7.76 | 4.46 | 155. | 27. | 0. | 0. | 36. | 163. | 190. | 190. |
| 261 | 4 | 3.11 | 4.54 | 162. | 28. | 0. | 0. | 37. | 171. | 199. | 199. |
| 271 | 4 | 3.77 | 4.54 | 168. | 28. | 0. | 0. | 38. | 178. | 206. | 206. |
| 281 | 4 | 6.65 | 4.45 | 174. | 28. | 0. | 0. | 39. | 184. | 212. | 212. |
| 291 | 4 | 7.21 | 4.36 | 178. | 28. | 0. | 0. | 41. | 190. | 218. | 218. |
| 301 | 4 | 7.19 | 4.39 | 184. | 28. | 0. | 0. | 42. | 197. | 225. | 225. |
| 311 | 4 | 2.74 | 4.31 | 189. | 30. | 0. | 0. | 45. | 203. | 233. | 233. |
| 321 | 4 | 3.56 | 4.33 | 194. | 32. | 0. | 0. | 47. | 208. | 240. | 240. |
| 331 | 4 | 6.75 | 4.40 | 201. | 32. | 0. | 0. | 47. | 215. | 247. | 247. |
| 341 | 4 | 7.74 | 4.39 | 206. | 34. | 0. | 0. | 50. | 221. | 255. | 255. |
| 351 | 4 | 3.43 | 4.32 | 209. | 35. | 0. | 0. | 52. | 226. | 261. | 261. |
| 361 | 4 | 7.91 | 4.37 | 216. | 36. | 0. | 0. | 53. | 232. | 268. | 268. |
| 371 | 4 | 7.76 | 4.38 | 220. | 39. | 0. | 0. | 56. | 236. | 275. | 275. |
| 381 | 4 | 0.08 | 4.34 | 225. | 40. | 0. | 0. | 58. | 242. | 282. | 282. |
| 391 | 4 | 7.11 | 4.24 | 230. | 43. | 0. | 0. | 60. | 246. | 289. | 289. |
| 401 | 4 | 7.11 | 4.22 | 235. | 44. | 0. | 0. | 62. | 252. | 296. | 296. |
| 411 | 4 | 7.58 | 4.26 | 240. | 45. | 0. | 0. | 64. | 258. | 303. | 303. |

FIGURE 4.3

ILLUSTRATING DETECTOR PHASE MARGIN WITH 75 kHz HPF

NUMBER OF TEST BITS 1000 HF CUT OFF, IN KHZ 150.0000 # SMPS. IN INT 3

PLL GAIN 36000. PLL BW 5300. INITIAL VCOPHASE(DEG) 45.

VALUE OF KOFF 3

DISPLACMENT FROM VCO TO DET. 0

DOPP OFFSET IN HZ (SW#7) 1000. DOPP RATE IN HZ/ SEC(SW#8) 0.

SAMPLED AMPLITUDE OF THE READ BEAM

| | | | | | | | | | | | |
|---|---|---|---|---|---|---|---|---|---|---|---|
| 0.000 | 0.000 | 0.000 | 0.000 | 0.000 | 0.000 | 0.000 | 0.000 | | | | |
| 0.000 | 0.000 | 0.000 | 0.000 | 0.000 | 0.000 | 0.000 | 0.000 | | | | |
| 0.000 | 0.000 | 0.000 | 0.000 | 0.030 | 0.050 | 0.130 | 0.110 | | | | |
| 0.060 | 0.410 | 0.710 | 0.960 | 0.960 | 0.710 | 0.410 | 0.060 | | | | |
| 0.110 | 0.130 | 0.050 | 0.030 | 0.000 | 0.000 | 0.000 | 0.000 | | | | |
| 0.000 | 0.000 | 0.000 | 0.000 | 0.000 | 0.000 | 0.000 | 0.000 | | | | |
| 0.000 | 0.000 | 0.000 | 0.000 | 0.000 | 0.000 | 0.000 | 0.000 | | | | |

| | | | | | | | | | | | |
|---|---|---|---|---|---|---|---|---|---|---|---|
| 1 | 4 | 3.50 | 4.50 | 0. | 0. | 0. | 0. | 0. | 0. | 0. | 0. |
| 11 | 4 | 3.30 | 4.30 | 7. | 0. | 0. | 0. | 0. | 7. | 7. | 7. |
| 21 | 4 | 6.20 | 4.34 | 12. | 0. | 0. | 1. | 3. | 14. | 14. | 15. |
| 31 | 4 | 5.34 | 4.31 | 13. | 0. | 0. | 3. | 8. | 20. | 20. | 24. |
| 41 | 4 | 7.35 | 4.33 | 17. | 0. | 0. | 5. | 12. | 28. | 28. | 33. |
| 51 | 4 | 7.64 | 4.24 | 21. | 0. | 0. | 5. | 16. | 36. | 36. | 41. |
| 61 | 4 | 7.63 | 4.25 | 25. | 0. | 0. | 8. | 19. | 43. | 43. | 51. |
| 71 | 4 | 7.05 | 4.29 | 30. | 0. | 1. | 9. | 22. | 51. | 52. | 60. |
| 81 | 4 | 3.08 | 4.26 | 32. | 0. | 2. | 12. | 26. | 58. | 60. | 70. |
| 91 | 4 | 7.37 | 4.22 | 39. | 0. | 2. | 13. | 28. | 66. | 68. | 79. |
| 101 | 4 | 7.33 | 4.31 | 46. | 0. | 2. | 13. | 30. | 75. | 77. | 88. |
| 111 | 4 | 7.83 | 4.32 | 48. | 0. | 3. | 17. | 34. | 81. | 84. | 98. |
| 121 | 4 | 7.84 | 4.30 | 50. | 0. | 3. | 18. | 39. | 88. | 91. | 106. |
| 131 | 4 | 5.46 | 4.40 | 55. | 0. | 4. | 20. | 41. | 95. | 99. | 116. |
| 141 | 4 | 3.46 | 4.48 | 58. | 0. | 5. | 22. | 46. | 103. | 108. | 1.. |
| 151 | 4 | 2.37 | 4.36 | 62. | 0. | 5. | 22. | 50. | 111. | 116. | 133. |
| 161 | 4 | 3.68 | 4.24 | 65. | 0. | 5. | 22. | 54. | 119. | 124. | 141. |
| 171 | 4 | 3.31 | 4.30 | 72. | 0. | 5. | 22. | 56. | 128. | 133. | 150. |
| 181 | 4 | 6.15 | 4.32 | 78. | 0. | 5. | 22. | 59. | 136. | 141. | 158. |
| 191 | 4 | 6.58 | 4.27 | 80. | 0. | 6. | 25. | 63. | 142. | 148. | 167. |
| 201 | 4 | 2.26 | 4.15 | 83. | 0. | 6. | 25. | 68. | 150. | 156. | 175. |
| 211 | 4 | 3.75 | 4.10 | 85. | 0. | 6. | 25. | 73. | 158. | 164. | 183. |
| 221 | 4 | 2.68 | 4.23 | 92. | 0. | 6. | 26. | 75. | 166. | 172. | 192. |
| 231 | 4 | 7.17 | 4.18 | 96. | 0. | 6. | 26. | 79. | 174. | 180. | 200. |
| 241 | 4 | 6.24 | 4.20 | 101. | 0. | 6. | 26. | 82. | 182. | 188. | 208. |
| 251 | 4 | 7.27 | 4.19 | 104. | 0. | 6. | 26. | 87. | 190. | 196. | 216. |
| 261 | 4 | 2.17 | 4.27 | 111. | 0. | 6. | 27. | 89. | 199. | 205. | 226. |
| 271 | 4 | 3.69 | 4.22 | 112. | 0. | 6. | 28. | 94. | 206. | 212. | 234. |
| 281 | 4 | 5.03 | 4.21 | 115. | 0. | 6. | 29. | 98. | 212. | 218. | 242. |
| 291 | 4 | 6.68 | 4.08 | 115. | 0. | 6. | 32. | 104. | 218. | 224. | 250. |
| 301 | 3 | 6.70 | 3.98 | 117. | 0. | 6. | 33. | 109. | 225. | 231. | 258. |
| 311 | 3 | 2.40 | 3.99 | 121. | 0. | 6. | 35. | 113. | 233. | 239. | 268. |
| 321 | 3 | 2.45 | 3.86 | 123. | 0. | 6. | 35. | 118. | 240. | 246. | 275. |
| 331 | 3 | 5.14 | 3.77 | 126. | 0. | 6. | 35. | 122. | 247. | 253. | 283. |
| 341 | 3 | 7.80 | 3.77 | 130. | 0. | 7. | 37. | 126. | 255. | 262. | 292. |
| 351 | 3 | 2.76 | 3.74 | 131. | 0. | 8. | 41. | 131. | 261. | 269. | 302. |
| 361 | 3 | 7.21 | 3.64 | 134. | 0. | 8. | 42. | 135. | 268. | 276. | 310. |
| 371 | 3 | 7.09 | 3.66 | 138. | 0. | 8. | 45. | 138. | 275. | 283. | 320. |
| 381 | 3 | 7.51 | 3.73 | 141. | 0. | 9. | 47. | 142. | 282. | 291. | 329. |
| 391 | 3 | 5.26 | 3.75 | 145. | 0. | 9. | 48. | 145. | 289. | 298. | 338. |
| 401 | 3 | 6.10 | 3.81 | 148. | 0. | 10. | 51. | 149. | 296. | 306. | 347. |
| 411 | 3 | 6.42 | 3.66 | 149. | 0. | 10. | 52. | 155. | 303. | 313. | 355. |

FIGURE 4.4

ILLUSTRATING DETECTOR PHASE MARGIN WITH 150 kHz HPF

NUMBER OF TEST BITS 1000 HF CUT OFF, IN KHZ 225.0000 # SMPS. IN INT 3

PLL GAIN 36000. PLL BW 5300. INITIAL VCOPHASE(DEG) 45.

VALUE OF KOFF 3

DISPLACMENT FROM VCO TO DET. 0

DOPP OFFSET IN HZ (SW#7) 1000. DOPP RATE IN HZ/ SEC(SW#8) 0.

SAMPLED AMPLITUDE OF THE READ BEAM

| | | | | | | | | | | | |
|---|---|---|---|---|---|---|---|---|---|---|---|
| 0.000 | 0.000 | 0.000 | 0.000 | 0.000 | 0.000 | 0.000 | 0.000 | | | | |
| 0.000 | 0.000 | 0.000 | 0.000 | 0.000 | 0.000 | 0.000 | 0.000 | | | | |
| 0.000 | 0.000 | 0.000 | 0.000 | 0.030 | 0.050 | 0.130 | 0.110 | | | | |
| 0.060 | 0.410 | 0.710 | 0.960 | 0.960 | 0.710 | 0.410 | 0.060 | | | | |
| 0.110 | 0.130 | 0.050 | 0.030 | 0.000 | 0.000 | 0.000 | 0.000 | | | | |
| 0.000 | 0.000 | 0.000 | 0.000 | 0.000 | 0.000 | 0.000 | 0.000 | | | | |
| 0.000 | 0.000 | 0.000 | 0.000 | 0.000 | 0.000 | 0.000 | 0.000 | | | | |

| | | | | | | | | | | | |
|---|---|---|---|---|---|---|---|---|---|---|---|
| 1 | 4 | 3.31 | 4.50 | 0. | 0. | 0. | 0. | 0. | 0. | 0. | 0. |
| 11 | 4 | 2.92 | 4.29 | 0. | 0. | 0. | 0. | 7. | 7. | 7. | 7. |
| 21 | 4 | 5.72 | 4.13 | 3. | 1. | 1. | 3. | 11. | 15. | 15. | 16. |
| 31 | 3 | 2.80 | 3.99 | 4. | 3. | 3. | 8. | 19. | 24. | 24. | 25. |
| 41 | 3 | 6.81 | 3.96 | 7. | 5. | 5. | 12. | 25. | 33. | 33. | 34. |
| 51 | 3 | 7.17 | 3.82 | 7. | 5. | 5. | 16. | 33. | 41. | 41. | 42. |
| 61 | 3 | 6.98 | 3.91 | 10. | 8. | 8. | 19. | 39. | 51. | 51. | 52. |
| 71 | 3 | 2.41 | 3.98 | 14. | 9. | 9. | 22. | 45. | 60. | 60. | 61. |
| 81 | 3 | 2.89 | 3.95 | 19. | 12. | 12. | 26. | 52. | 70. | 70. | 70. |
| 91 | 3 | 6.91 | 3.90 | 24. | 13. | 13. | 28. | 58. | 79. | 79. | 80. |
| 101 | 3 | 2.80 | 3.92 | 25. | 13. | 13. | 30. | 66. | 88. | 88. | 89. |
| 111 | 3 | 7.22 | 3.84 | 31. | 17. | 17. | 34. | 74. | 98. | 98. | 99. |
| 121 | 3 | 7.13 | 3.87 | 33. | 18. | 18. | 39. | 81. | 106. | 106. | 107. |
| 131 | 3 | 2.27 | 3.91 | 37. | 20. | 20. | 41. | 87. | 116. | 116. | 117. |
| 141 | 3 | 2.95 | 4.00 | 41. | 22. | 22. | 46. | 94 | 125. | 125. | 125. |
| 151 | 3 | 1.53 | 3.94 | 42. | 22. | 22. | 50. | 101. | 133. | 133. | 133. |
| 161 | 3 | 3.22 | 3.93 | 43. | 22. | 22. | 54. | 107. | 141. | 141. | 141. |
| 171 | 3 | 2.92 | 3.93 | 45. | 22. | 22. | 56. | 115. | 150. | 150. | 150. |
| 181 | 4 | 2.64 | 4.00 | 48. | 22. | 22. | 59. | 120. | 158. | 158. | 159. |
| 191 | 3 | 5.83 | 3.96 | 53. | 25. | 25. | 63. | 127. | 167. | 167. | 168. |
| 201 | 3 | 1.70 | 3.99 | 55. | 25. | 25. | 68. | 133. | 175. | 175. | 176. |
| 211 | 4 | 3.23 | 4.03 | 57. | 25. | 25. | 73. | 136. | 183. | 183. | 183. |
| 221 | 3 | 1.34 | 3.87 | 61. | 26. | 26. | 75. | 145. | 192. | 192. | 193. |
| 231 | 3 | 6.95 | 3.93 | 65. | 26. | 26. | 79. | 149. | 200. | 200. | 201. |
| 241 | 4 | 5.71 | 4.05 | 68. | 26. | 26. | 82. | 154. | 208. | 208. | 209. |
| 251 | 4 | 6.82 | 4.04 | 70. | 26. | 26. | 87. | 160. | 216. | 216. | 217. |
| 261 | 3 | 1.46 | 3.98 | 74. | 27. | 27. | 89. | 167. | 226. | 226. | 226. |
| 271 | 3 | 3.24 | 3.92 | 76. | 28. | 28. | 94. | 173. | 234. | 234. | 234. |
| 281 | 3 | 2.47 | 3.87 | 79. | 29. | 29. | 98. | 180. | 242. | 242. | 243. |
| 291 | 3 | 5.84 | 3.77 | 82. | 32. | 32. | 104. | 188. | 250. | 250. | 251. |
| 301 | 3 | 5.83 | 3.79 | 84. | 33. | 33. | 109. | 195. | 258. | 258. | 259. |
| 311 | 3 | 1.91 | 3.88 | 89. | 35. | 35. | 113. | 202. | 268. | 268. | 268. |
| 321 | 3 | 1.40 | 3.87 | 91. | 35. | 35. | 118. | 207. | 275. | 275. | 276. |
| 331 | 3 | 2.42 | 3.89 | 93. | 35. | 35. | 122. | 213. | 283. | 283. | 284. |
| 341 | 3 | 2.99 | 3.95 | 99. | 37. | 37. | 126. | 218. | 292. | 292. | 293. |
| 351 | 4 | 1.61 | 4.01 | 102. | 41. | 41. | 131. | 227. | 302. | 302. | 302. |
| 361 | 3 | 2.83 | 3.95 | 105. | 42. | 42. | 135. | 233. | 310. | 310. | 311. |
| 371 | 3 | 6.69 | 3.99 | 108. | 45. | 45. | 138. | 239. | 320. | 320. | 321. |
| 381 | 3 | 7.14 | 3.95 | 112. | 47. | 47. | 142. | 246. | 329. | 329. | 330. |
| 391 | 3 | 2.42 | 3.98 | 117. | 48. | 48. | 145. | 251. | 338. | 338. | 339. |
| 401 | 3 | 5.51 | 3.97 | 123. | 51. | 51. | 149. | 257. | 347. | 347. | 348. |
| 411 | 3 | 2.96 | 3.89 | 125. | 52. | 52. | 155. | 264. | 355. | 355. | 356. |

FIGURE 4.5

ILLUSTRATING DETECTOR PHASE MARGIN WITH 225 kHz HPF

NUMBER OF TEST BITS 1000 HF CUT OFF, IN KHZ 20.0000 # SMPS. IN INT 5

PLL GAIN 36000. PLL BW 5300. INITIAL VCOPHASE(DEG) 135.

VALUE OF KOFF 3

DISPLACMENT FROM VCO TO DET. 0

DOPP OFFSET IN HZ (SW#7) 1000. DOPP RATE IN HZ/ SEC(SW#8) 0.

SAMPLED AMPLITUDE OF THE READ BEAM

| | | | | | | | | | | | |
|---|---|---|---|---|---|---|---|---|---|---|---|
| 0.000 | 0.000 | 0.000 | 0.000 | 0.000 | 0.000 | 0.000 | 0.000 | | | | |
| 0.000 | 0.000 | 0.000 | 0.000 | 0.000 | 0.000 | 0.000 | 0.000 | | | | |
| 0.000 | 0.000 | 0.000 | 0.000 | 0.000 | 0.000 | 0.000 | 0.000 | | | | |
| 1.000 | 1.000 | 1.000 | 1.000 | 1.000 | 1.000 | 1.000 | 1.000 | | | | |
| 0.000 | 0.000 | 0.000 | 0.000 | 0.000 | 0.000 | 0.000 | 0.000 | | | | |
| 0.000 | 0.000 | 0.000 | 0.000 | 0.000 | 0.000 | 0.000 | 0.000 | | | | |
| 0.000 | 0.000 | 0.000 | 0.000 | 0.000 | 0.000 | 0.000 | 0.000 | | | | |

| | | | | | | | | | | | |
|---|---|---|---|---|---|---|---|---|---|---|---|
| 1 | 3 | 0.00 | 3.50 | 0. | 0. | 0. | 0. | 0. | 0. | 0. | 0. |
| 11 | 3 | 3.85 | 3.59 | 7. | 0. | 0. | 0. | 0. | 7. | 7. | 7. |
| 21 | 3 | 7.81 | 3.73 | 15. | 3. | 0. | 0. | 0. | 11. | 14. | 14. |
| 31 | 3 | 7.38 | 3.93 | 21. | 3. | 0. | 0. | 0. | 17. | 20. | 20. |
| 41 | 4 | 7.43 | 4.07 | 27. | 7. | 0. | 0. | 2. | 21. | 28. | 28. |
| 51 | 4 | 7.85 | 4.32 | 35. | 10. | 0. | 0. | 2. | 26. | 36. | 36. |
| 61 | 4 | 0.87 | 4.50 | 41. | 12. | 0. | 0. | 3. | 31. | 43. | 43. |
| 71 | 4 | 7.83 | 4.72 | 48. | 14. | 0. | 0. | 4. | 37. | 51. | 51. |
| 81 | 4 | 3.65 | 4.85 | 54. | 15. | 0. | 0. | 4. | 43. | 58. | 58. |
| 91 | 4 | 7.80 | 4.91 | 63. | 16. | 0. | 0. | 4. | 50. | 66. | 66. |
| 101 | 4 | 7.87 | 4.85 | 72. | 16. | 0. | 0. | 4. | 59. | 75. | 75. |
| 111 | 4 | 0.04 | 4.70 | 78. | 17. | 0. | 0. | 4. | 64. | 81. | 81. |
| 121 | 4 | 7.95 | 4.69 | 85. | 20. | 0. | 0. | 4. | 68. | 88. | 88. |
| 131 | 4 | 7.49 | 4.68 | 92. | 22. | 0. | 0. | 4. | 73. | 95. | 95. |
| 141 | 4 | 3.32 | 4.58 | 99. | 25. | 0. | 0. | 4. | 78. | 103. | 103. |
| 151 | 4 | 3.22 | 4.53 | 107. | 29. | 0. | 0. | 4. | 82. | 111. | 111. |
| 161 | 4 | 3.69 | 4.50 | 115. | 33. | 0. | 0. | 4. | 86. | 119. | 119. |
| 171 | 4 | 3.88 | 4.72 | 124. | 33. | 0. | 0. | 4. | 95. | 128. | 128. |
| 181 | 4 | 7.90 | 4.82 | 133. | 35. | 0. | 0. | 4. | 101. | 136. | 136. |
| 191 | 4 | 7.61 | 4.75 | 139. | 36. | 0. | 0. | 4. | 106. | 142. | 142. |
| 201 | 4 | 3.50 | 4.74 | 147. | 37. | 0. | 0. | 4. | 113. | 150. | 150. |
| 211 | 4 | 3.72 | 4.74 | 154. | 39. | 0. | 0. | 4. | 119. | 158. | 158. |
| 221 | 4 | 7.43 | 4.75 | 163. | 39. | 0. | 0. | 4. | 127. | 166. | 166. |
| 231 | 4 | 7.76 | 4.76 | 171. | 40. | 0. | 0. | 4. | 134. | 174. | 174. |
| 241 | 4 | 7.63 | 4.79 | 179. | 42. | 0. | 0. | 4. | 140. | 182. | 182. |
| 251 | 4 | 0.05 | 4.83 | 187. | 43. | 0. | 0. | 4. | 147. | 190. | 190. |
| 261 | 4 | 3.98 | 4.85 | 195. | 47. | 0. | 0. | 4. | 152. | 199. | 199. |
| 271 | 4 | 3.92 | 4.87 | 202. | 47. | 0. | 0. | 4. | 159. | 206. | 206. |
| 281 | 4 | 7.49 | 4.69 | 209. | 48. | 0. | 0. | 4. | 164. | 212. | 212. |
| 291 | 4 | 7.54 | 4.75 | 215. | 48. | 0. | 0. | 4. | 170. | 218. | 218. |
| 301 | 4 | 7.60 | 4.68 | 222. | 49. | 0. | 0. | 4. | 176. | 225. | 225. |
| 311 | 4 | 3.07 | 4.67 | 229. | 52. | 0. | 0. | 4. | 181. | 233. | 233. |
| 321 | 4 | 3.93 | 4.64 | 237. | 54. | 0. | 0. | 4. | 186. | 240. | 240. |
| 331 | 4 | 7.19 | 4.70 | 244. | 57. | 0. | 0. | 4. | 190. | 247. | 247. |
| 341 | 4 | 7.85 | 4.75 | 252. | 58. | 0. | 0. | 4. | 197. | 255. | 255. |
| 351 | 4 | 4.19 | 4.78 | 257. | 60. | 0. | 0. | 4. | 200. | 261. | 261. |
| 361 | 4 | 0.07 | 4.74 | 265. | 64. | 0. | 0. | 4. | 204. | 268. | 268. |
| 371 | 4 | 0.90 | 4.74 | 269. | 67. | 1. | 0. | 7. | 208. | 274. | 275. |
| 381 | 4 | 7.73 | 4.72 | 274. | 71. | 2. | 0. | 9. | 211. | 280. | 282. |
| 391 | 4 | 7.40 | 4.71 | 281. | 73. | 2. | 0. | 9. | 216. | 287. | 289. |
| 401 | 4 | 7.77 | 4.75 | 288. | 74. | 2. | 0. | 9. | 222. | 294. | 296. |
| 411 | 4 | 0.14 | 4.80 | 295. | 76. | 2. | 0. | 9. | 227. | 301. | 303. |

FIGURE 4.6
SYSTEM PERFORMANCE WITH "RECTANGULAR" BEAM PROFILE

## 5.0 SOME IMPLEMENTATION CONSIDERATIONS

A block diagram of the demodulator is given in Figure 5.1. The following points about the implementation are worth noting. First, we note that typically the VCO should run at twice the bit rate (2 x 4/3 MHz) to accommodate the Miller modulation. We plan, however, to run at 6 x 4/3 MHz and divide by 3 as shown in Figure 5.1. This will allow us to provide a synchronous data clock, 3xCK, to the decoder at three times the data rate* (in addition to the normal clock, DATACK, at the data rate). Secondly, we plan to use a crystal VCO in the initial design (Greenray Model N-412, or equivalent). Such a VCO can be pulled by $\pm 0.1\%$ (which is only slightly more than we require to handle disc eccentricity), and at the same time maintain its center frequency to within $\pm 0.005\%$ from $0^{\circ}$ to $50^{\circ}$C. We note that, regardless of the type of VCO selected, its center frequency must remain within about $\pm 8$ to 10 kHz of the nominal value. Otherwise, the loop bandwidth becomes excessively large just to accommodate the VCO error. The VCO output will contain a lot of jitter under these conditions, and simulations showed the 8 to 10 kHz figure to about the maximum allowable.

To resolve the clock phase ambiguity resulting from the Miller encoding, the demodulator will continuously test the output data clock to determine that it is the correct phase (of the two possible). If and when this test indicates that the phase is incorrect, it will automatically select the opposite one. This test can be understood by observing from Figure 2.1 that if the incorrect sampling phase is used, an isolated zero will result in four samples of the same polarity. With the correct sampling phase, four identical sample polarities in two consecutive baud times can never occur. With the incorrect phase, it will occur on an average of about one out of eight consecutive baud pairs. A 64-state counter will initially be set to state 32 and, on each consecutive bit pair examined, will count up by one, if all four polarities are not the same, or down by 16 otherwise.** If and when the counter state exceeds 48, the DATA ENABLE line goes high. Similarly, on any baud pair

---

*Lorend Vries has indicated that this rate is required for his decoder.

**An attempt to count below state 1 (above state 64) causes the counter to go to state 1 (64).

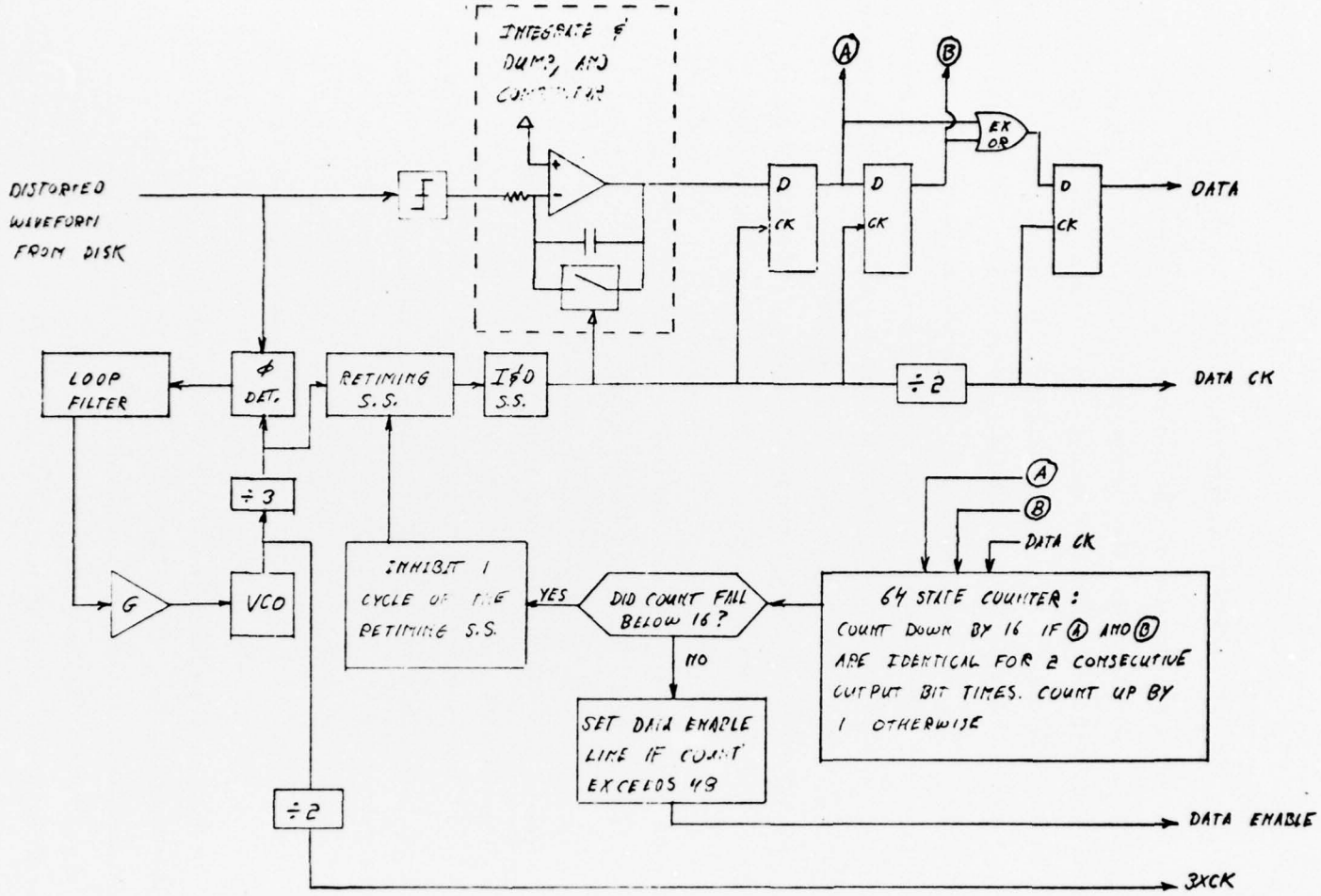


FIGURE 5.1

DEMODULATOR HARDWARE BLOCK DIAGRAM

for which the state goes from *above* to *below* 16, the opposite demodulation phase is selected. With this type of test, an incorrect phase will be recognized and corrected quickly. We note that, regardless of the state of the DATA ENABLE line, we will continue to provide DATA, DATACK, and 3XCK to the decoder.

Selection of the opposite demodulation phase (when the state falls below 16) can be achieved by inhibiting a *single* firing of the retiming single-shot shown in Figure 5.1. (This retiming single-shot is provided to compensate for delays introduced by the highpass filter used to eliminate laser noise, and was discussed at the end of the previous section.)

Twice per baud (i.e., once in each half of the baud), the edge out of the retiming single-shot fires the integrate-and-dump (I&D) single-short. During the time out of the I&D SS, the bandlimited waveform is integrated in an RC network, and sampled by a comparator at the dump time. The resulting TTL level of the comparator output is clocked into the two-stage shift registers which are exclusive-ORed to determine the output data bit polarity.

Finally, we note that in this report we have assumed the bit rate read from the disc was 4/3 MHz. As a result of the meeting at GAC on 12 December 1976 (Kenney, Nadan, Stoller, Harper and Goutmann), it was decided to increase this rate to 1.67 MHz. The purpose of this increase was to accommodate overhead which will be required in any commercial peripheral application. The demodulator hardware being built by GAC will be designed to operate at the 1.67 MHz rate, and we are confident that the analysis results concluded for the 4/3 MHz rate remain essentially unchanged at the 1.67 MHz rate.

## APPENDIX A

## ASSUMPTIONS MADE IN DERIVING THE CONVOLUTION OF FIGURE 2.3

When the read beam passes over a pit, it creates a pulse, $p(t)$, out of the photo detector, where $p(t)$ is the convolution of the beam shape and the reflecting "profile" of the pit. To write a sinewave of frequency f onto the disc, we assume that pits are written at a periodic spacing of $\tau = 1/f$. Consequently, if the Fourier transform of $p(t)$ is given by $P(\omega)$, the spectrum of the periodic sequence is $P(\omega)$ evaluated at the frequencies $n\Delta f$ ($\Delta f = 1/\tau$, and for an even convolution function, n takes on only odd values). The fundamental (n=1) corresponds to the "frequency response" of the disc and is given by $P(2\pi f)$.

To obtain Figure 2.3, points were picked off from Figure 12 of reference 3 at 1 MHz increments, and a 32-point $FFT^{-1}$ on the resulting array was performed. Consequently, the resulting samples of $p(t)$ are separated by 1/32 of a microsecond (.03125 μs). Since Figure 12 of reference 3 corresponds to a disc rotational speed of 30 Hz, and an inner diameter of 110 mm, 0.03125 μs corresponds to 0.321 microns. Samples of the inverse FFT plotted at increments of 0.321 microns appear as the broken curve of Figure 2.3.

The solid curve of Figure 2.3 is obtained by convolving the sampled data version of the pit scattering profile: (1,1,1,1,1,1,1,1) with the sampled beam amplitudes taken from Figure 2.2 at a spacing of $1.0\alpha$: (0.03, 0.05, 0.13, 0.11, 0.06, 0.41, 0.71, 0.96, 0.96, 0.71, 0.41, 0.06, 0.11, 0.13, 0.05, 0.03). Since the pit size is 0.99 microns, samples of the convolved waveform are spaced at intervals of 0.99/8 = 0.127 micron.

# APPENDIX B

## FORTRAN LISTING OF SIMULATION PROGRAM

```
FORTRAN IV      V01C-03A                                        PAGE 001

0001            DIMENSION ACCC(8),IN(8),BEAM(56)
0002            DIMENSION INDAT(64),XOUT(64),POS(8)
0003            DATA POS/8*0./
0004            DATA ACCC/8*0./
0005            DATA BEAM/0.,0.,0.,0.,0.,0.,0.,0.,0.,0.,0.,0.,0.,0.,0.,0.,
               *0.,0.,0.,0.,.03,.05,.13,.11,.06,.41,.71,.96,
               *.96,.71,.41,.06,.11,.13,.05,.03,0.,0.,0.,0.,
               *.0,.0,.0,.0,.0,.0,.0,.0,.0,.0,.0,.0,.0,.0,.0,.0,.0,.0,.0,.0/
0006            COMPLEX P,AL,ZP
0007            ACCEPT 99,NBITS,LNGTH,KOFF,HFCUT,GAIN,BW,PHI,IDOFF,VOL,ACC
0008    99      FORMAT(3I5,4F10.2,I5,2F10.2)
0009            PRINT 22,NBITS,HFCUT,LNGTH
0010    22      FORMAT(1HO,'  NUMBER OF TEST BITS',I7,'  HF CUT OFF,IN KHZ',F10.4,
               *' # SMPS.  IN INT',I5)
0011            PRINT 63,GAIN,BW,PHI
0012    63      FORMAT(1HO,' PLL GAIN',F10.0,'     PLL BW',F10.0,'     INITIAL VCO
               *PHASE(DEG)',F10.0)
0013            PRINT 62,KOFF
0014    62      FORMAT(1HO,'     VALUE OF KOFF',I8)
0015            PRINT 64,IDOFF
0016    64      FORMAT(1HO,'  DISPLACMENT FROM VCO TO DET.',I10)
0017            PRINT 65,VOL,ACC
0018    65      FORMAT(1HO,' DOPP OFFSET IN HZ (SW#7)',F10.0,' DOPP RATE IN HZ/
               *SEC(SW#8)',F10.0)
0019            PRINT 66
0020    66      FORMAT(1HO,'  SAMPLED AMPLITUDE OF THE READ BEAM')
0021            PRINT 67,BEAM
0022    67      FORMAT(8F10.3)
0023            ICC=10
0024            FSTVOL=1.
0025            P=(-.707107,.707107)
0026            SR=((4./3.)*10.**6)*8.
0027            DELPHI=6.28319/4.
0028            XXX=VOL*6.28319/SR
0029            WN=6.28319*BW
0030            ZETA=.707
0031            TT=WN*WN/GAIN
0032            TT=1./TT
0033            T2=(2.*ZETA/WN)-(1./GAIN)
0034            RCH=1./(2.*SR)
0035            CON=(T2+RCH)/(TT+RCH)
0036            ZZL=(T2-RCH)/(T2+RCH)
0037            ZPL=(TT-RCH)/(TT+RCH)
0038            PHI=PHI*6.28319/360.
0039            OUTN=0.
0040            FIN=0.
0041            FX1=0.
0042    52      FORMAT(2I5)
0043            WCUT=6.28319*HFCUT*(10.**3)
0044            AL=WCUT/(2.*SR*P)
0045            CO=REAL((1.-AL)*(1.-CONJG(AL)))
0046            CO=1./CO
0047            ZP=(1.+AL)/(1.-AL)
0048            C2=2.*REAL(ZP)
```

INITIALIZATION AND SETUP

```
0049          C3=REAL(ZP*CONJG(ZP))
0050          X2=0.
0051          X1=0.
0052          JSEED=0
0053          ISEED=0
0054          DO 80 I=1,7
0055    80    IN(I)=-1
0056          DO 81 I=1,8
0057          INDAT(I)=-1
0058          INDAT(I+8)=1
0059          INDAT(I+16)=-1
0060          INDAT(I+24)=1
0061          INDAT(I+32)=-1
0062          INDAT(I+40)=1
0063    81    INDAT(I+48)=-1
0064          INI=7
0065          LSAMP=-1
0066          II=56
0067          DO 19 JBITS=1,NBITS
0068          PVOL=0.
0069          FIRST=1.
0070          INP=INI
0071          INI=MOD(INI,8)+1
0072          INT=MOD(INI+KOFF,8)+1
0073          IN(INI)=-1
0074          X=RAN(ISEED,JSEED)
0075          IF(X.LE.0.5)GO TO 3
0077          IN(INI)=1
0078          DO 4 IX=1,8
0079          IF(IX.EQ.5)LSAMP=-LSAMP
0081          II=MOD(II,64)+1
0082    4     INDAT(II)=LSAMP
0083          GO TO 5
0084    3     IF(IN(INP).EQ.-1)GO TO 6
0086    8     DO 7 IX=1,8
0087          II=MOD(II,64)+1
0088    7     INDAT(II)=LSAMP
0089          GO TO 5
0090    6     LSAMP=-LSAMP
0091          GO TO 8
0092    5     JS1=MOD(II,64)
0093          DO 11 JCONV=1,8
0094          JS1=MOD(JS1,64)+1
0095          IS1=JS1
0096          XIN=0.
0097          DO 12 I=1,56
0098          IS1=MOD(IS1,64)+1
0099    12    XIN=XIN+(FLOAT(INDAT(IS1)))*BEAM(I)
0100          X3=X2
0101          X2=X1
0102          X1=C2*X2-C3*X3+C0*XIN
0103          OUTP=OUTN
0104          OUTN=X1-2.*X2+X3
0105          CALL SSWTCH(5,JUMP)
```

INITIALIZATION AND SETUP

SELECT RANDOM NRZ DATA BIT AND PERFORM MILLER ENCODING

CONVOLVE BEAM AND PIT

TWO-POLE BUTTERWORTH HPF

```
0106        IF(JUMP.NE.2)PRINT 70,OUTN,JS1,JBITS,IN(INI),II
0108   70   FORMAT(F10.2,4I6)
0109        XOUT(JS1)=OUTN
0110        IF(SIGN(1.,OUTP).EQ.SIGN(1.,OUTN))GO TO 51
0112        ACCC(JCONV)=ACCC(JCONV)+1
0113        YY=ABS(OUTP)/(ABS(OUTN)+ABS(OUTP))
0114        FIJK=FLOAT(JCONV)-(1.-YY)
0115        FIN=(PHI+DELPHI*YY)-3.14159
0116        IF(FIN.GT.3.14159)FIN=FIN-6.28319
0118   51   FX2=FX1
0119        FX1=CON*FIN+ZPL*FX2
0120        FOUT=FX1-FX2*ZZL
0121        CALL SSWTCH(7,JUMP)
0122        IF(JUMP.EQ.2)GO TO 94
0124        PVOL=1.
0125        IF(FSTVOL.EQ.1)PRINT 150
0127        FSTVOL=0.
0128  150   FORMAT(1H0,'  FREQ STEP STARTS HERE')
0129   94   PHI=PHI+DELPHI+(GAIN*FOUT/SR)+PVOL*XXX
0130        IF(PHI.LT.6.28319)GO TO 11
0132        IICON=MOD(JCONV,8)+1
0133        EX=FLOAT(IICON)-((PHI-6.28319)/DELPHI)
0134        IF(FIRST.NE.1.)GO TO 11
0136        FIRST=0.
0137        IJK=MOD(JCONV+IDOFF,8)
0138        CALL SSWTCH(2,JUMP)
0139        IF(JUMP.EQ.2)GO TO 11
0141        IF(ICC.EQ.10)GO TO 92
0143        ICC=ICC+1
0144        GO TO 11
0145   92   PRINT 91,JBITS,JCONV,FIJK,EX,POS
0146        ICC=1
0147   91   FORMAT(2I7,2F6.2,8F6.0)
0148   11   PHI=AMOD(PHI,6.28319)
0149   13   JS1=MOD(II+56,64)+1
0150        JS2=MOD(II+60,64)+1
0151   31   IF(JBITS.LE.3)GO TO 160
0153        DO 16 J=1,8
0154        JS1=MOD(JS1,64)+1
0155        JS2=MOD(JS2,64)+1
0156        IS1=JS1
0157        IS2=JS2
0158        S1=0.
0159        S2=0
0160        DO 32 K=1,LNGTH
0161        S1=S1+SIGN(1.,XOUT(IS1))
0162        S2=S2+SIGN(1.,XOUT(IS2))
0163        IS1=MOD(IS1,64)+1
0164   32   IS2=MOD(IS2,64)+1
0165        CALL SSWTCH(3,JUMP)
0166        IF(JUMP.NE.2)PRINT 53,JS1,IS1,S1,S2,IN(INT)
0168   53   FORMAT(I20,I5,2F10.2,I6)
0169        IF(SIGN(1.,S1).NE.SIGN(1.,S2))GO TO 17
0171        GO TO 18
```

PHASE LOCK LOOP (Statements directly implementing the PLL are indicated with a check (✓). Other statements set up printout.

DETECTOR OPERATION

```
0172    17    IF(IN(INT).EQ.1)GO TO 16
0174          POS(J)=POS(J)+1.
0175          GO TO 16
0176    18    IF(IN(INT).EQ.-1)GO TO 16
0178          POS(J)=POS(J)+1.
0179    16    CONTINUE
0180          CALL SSWTCH(4,JUMP)
0181          IF(JUMP.NE.2)PRINT 54,POS
0183    54    FORMAT(8F6.1)
0184    160   CONTINUE
0185    19    CONTINUE
0186    24    FORMAT(8F6.0)
0187          PRINT 24,POS
0188          PRINT 24,ACCC
0189          CALL EXIT
0190          END
```

DETECTOR OPERATION (continued)

## REFERENCES


(1) Silver, Samuel (ed.), *Microwave Antenna Theory and Design*, Dover Publications, 1965, Section 6.8.

(2) Frank, N.H., *Introduction to Electricity and Optics*, McGraw-Hill Book Co., New York, 1940.

(3) Bōgels, P.W., *et al*, "System Coding Parameters, Mechanics and Electro-Mechanics of the Reflective Video Disk Player," presented at the IEEE 17th Chicago Spring Conference on Consumer Electronics, 8 June 1976.

(4) Gardner, F.M., *Phaselock Techniques*, John Wiley and Sons, New York, 1966.